DEPARTMENT OF ELECTRICAL AND ELECTRONIC ENGINEERING

3rd Year Individual Investigative Design Project BENG

Design of a Wound-Field Synchronous Reluctance Motor for Traction Applications

Project Supervisor: Professor Zi-Qiang Zhu

Second Marker: Professor Jiabin Wang

May 2013

Fraz Anwar Makki

Registration Number: 100239975

Word count: 5974 (excluding abstract and appendix)

ACKNOWLEDGEMENT

I would like to give a special thanks to Professor Zi-Qiang Zhu and Professor Jiabin Wang for all the help and guidance provided during the duration of this project. Secondly I would like to thank all of the PhD students that helped me to understand the concepts of operating the design software and helping me resolve the many issues I encountered throughout my project. Lastly I would like to thank the Electric Machines and Drives group and also the University of Sheffield for the usage of the laboratory space throughout the practical work on the project.

ABSTRACT

In this thesis the design of a wound-field synchronous reluctance motor (WFSRM) will be done using a software called Flux 2D and this design will be simulated and analysed using the software. This is being done in order to determine if a WFSRM machine type is a possible contender in hybrid vehicle and traction applications. This design will also be compared with the brushless IPM machine found in the Toyota Prius from which the WFSRM design is also inspired from.

CONTENTS

1. INTRODUCTION

1.1 Background

In recent years there has been a growing research in environment friendly energy sources such as wind energy and solar energy. This is due to a growing awareness in global warming and the need to reduce carbon emissions. All types of different industries are giving an interest in these ‘green’ energy sources. The automotive industry is no exception. This is due to the fact majority of the carbon emissions are in fact due to automobiles that use fossil fuels to run. Automotive manufacturers have been doing lots of research in the past few years in order to discover the best possible replacement and their research has yielded results such as fuel cells and electric motors to drive automobiles. Nowadays it is thought that electric hybrid vehicles are the future.

This thesis will focus on designing a possible electric motor design for automotive and traction applications of the wound-field synchronous reluctance machine type. This machine is inspired from the Toyota Prius hybrid vehicle electric motor which is a brushless IPM machine type. This existing machine will be modified by changing its rotor topology from a brushless IPM type to a wound-field synchronous reluctance type. The wound-field synchronous reluctance motor (WFSRM) will be designed and simulated using a software called Flux 2D and then the results will be compared with the Prius IPM motor specifications in order to determine how viable is a WFSRM machine for use in a hybrid vehicle.

1.2 Project Objectives

The main purpose of this design project is to design a wound-field synchronous reluctance motor (WFSRM) on a finite element analysis software called flux 2D. Using this software it is possible to do the machine analysis and obtain results. These results will then be compared with the results for the Prius machine and therefore it would be possible to state which type of machine would be better for the electric hybrid application at different operating conditions and how each of these individual machines be optimized to achieve maximum efficiency.

In general the machine stator design is identical to that of the Prius machine, however the rotor topology is altered and remade to that of the WFSRM type.

1.3 Basic theory of wound field synchronous reluctance machines

The basic WFSRM machine has the conventional three phase windings that are sinusoidally distributed on the machine stator. The word synchronous emphasises the fact that the supply voltages of the machine at all three phases must have the same magnitude, phase rotation and frequency. In a synchronous motor energy conversion can only take place if the rotor and stator fields are synchronised. The motor is running at synchronous speed when the rotor turns at exactly the same rate as the stators rotating magnetic field.

The fact the machine is a synchronous machine also emphasises that the stator produces a sinusoidally distributed magneto-motive force (mmf) in the air-gap of the motor under steady state conditions. The rotor will therefore rotate in synchronism with the field produced in the air-gap.

The WFSRM has a flux source in the rotor itself. Flux in the WFSRM machine is produced by giving DC current to the wound-field around the WFSRM rotor. An inverter drive is used to stabilize the WFSRM when running and also to start it. One of the advantages of a WFSRM machine is the fact that it does not require a squirrel-cage and therefore the motor can be optimized for maximum torque and power[1][2].

1.3 Cedrat Flux 2D functions

The software used to design the machine and to carry out all the simulations is called Flux 2D from Cedrat and for the entirety of the project version 11.1 of the software was used. This version had the advantage over previous versions of the software in having a built in ‘sketcher’ feature which enabled to be able to design the machine quickly by using lines and shapes without needing to do lengthy calculations and find coordinates in order to make the design as was the case in previous versions. This sketcher feature enabled to get the first thing required to test the WFSRM design and that is the geometry.

The geometry is basically the machine fully designed and ready to be meshed and analysed. The second stage was to build and assign ‘faces’ to ‘face regions’. What this means is that various regions in the machine geometry are assigned as faces and then these faces are assigned their relative properties. For example the rotor windings were assigned to its unique region, similarly the rotor and stator were assigned as regions of their own. Once faces are assigned to each region, the geometry is meshed and the application is defined.

Defining the application, in this case transmagnetic 2D analysis, enabled to define mechanical sets, import materials and assign properties to the face regions. For example the rotor and stator were assigned as magnetic non-conducting regions with the material used assigned as electrical steel. Similarly rotor and stator windings were assigned as coil conductor regions with the number of turns assigned using the same feature set. Mechanical sets allowed to split the machine geometry into two parts, a rotor and stator. The mechanical sets included the properties of these two entities. In case of the stator it was given a movement property of being ‘fixed’ so to ensure it is the stationary part of the machine. The rotor in turn was given the property to be able to rotate along an axis and using this feature set it was possible to set the speed in RPM and also the starting position of the rotor. Further features included the ability to set the friction coefficients of the machine but these were assumed negligible.

Once all of these tasks are carried out it is possible to create a solving scenario and perform the simulation of the geometry. Once the simulation is carried out it is possible to use built-in post-processing functions of the Flux 2D software in order to carry out various calculations such as cogging torque, air-gap flux density etc.

As mentioned before, before any simulation can take place, the geometry has to be 'meshed'. This is of particular importance as the mesh quality will directly relate to how accurate and precise the results obtained are. The mesh is divided into excellent quality elements, good quality elements, bad quality elements and poor quality elements. Practically it is desired to have over 99.8% of excellent quality elements and 0% poor quality elements, ideally it would be desired a 100% excellent quality mesh elements but this is not possible practically.

2. DESIGN METHODOLOGY

2.1 Design specifications

Table 2.1 shows the initial design specification for the WFSRM motor that will be tested and simulated on flux 2D.

Parameter	***Value***
Motor diameter	310 mm
Stator outer diameter	264 mm
Stator inner diameter	161.9 mm
Number of stator slots	48
Stator construction material	Steel
Rotor outer diameter	160.4 mm
Rotor inner diameter	95 mm
Number of rotor poles	8
Rotor construction material	Steel
Shaft diameter	90 mm
Air-gap	0.73 mm
Rotor winding material	Copper
Number of turns per coil	50
DC current input to coil	30 A
Number of turns in stator winding	26
Rated torque (Prius)	207 Nm
Maximum rated speed	13500 RPM
Maximum rated phase current (Prius)	167 A_{RMS}
Slot fill	47%
Rated maximum current density (Prius)	26 A/mm^2

Table 2.1

2.2 Important design factors

When deciding the design topology of the machine, there are three major parts to investigate for and these are the rotor, stator and air-gap. Some of the most critical design decisions are listed below:

- Choice of rotor winding material
- Choice of the number of turns for the rotor winding
- The air-gap length (l_g)
- The air-gap area (A_g)
- The rotor coil winding area (A_c)
- The material used for the construction of the stator and rotor

For example, the air-gap length, l_g, is important to consider because it directly affects the overall machine production cost. The smaller the air-gap chosen the more expensive will it be to manufacture the machine. The air-gap area is also important to consider because the magnetic flux is focussed through the air-gap from the rotor to stator and to have an efficient distribution of magnetic flux the air-gap area is critical.

The choice of material for the different parts of the machine is important because it will determine the overall efficiency and performance of the machine. Also the hysteresis and eddy current losses that materials exhibit will determine the overall electric loading (Q) and magnetic loading (B) of the machine and ideally we would want the electric and magnetic loading to be high because these two factors are directly related to the amount of torque that can be extracted from the machine.

Another important design parameter for the machine is the split ratio which is defined as the ratio between the rotor outer diameter (D_R) and stator outer diameter (D_S) and normally ranges from 0.5-0.7 in value. This is the optimum range of split ratio for designing electrical machines. For the WFSRM design discussed it is 0.61[3].

2.3 Stator design

The design of the stator of the WFSRM machine was based on the stator design of the IPM machine in the Toyota Prius. Its dimensions have been listed in table 2.1. Figure 2.1 shows the general stator slot design and table 2.2 shows the stator slot measurements.

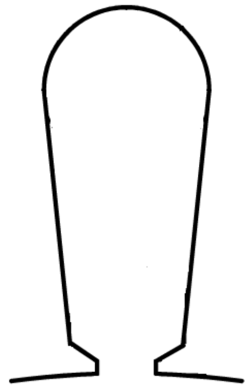

Figure 2.1

Parameter	***Value***
Stator outer diameter	264mm
Stator inner diameter	161.90mm
Stack length	50.8mm
Slot opening	1.88mm
Slot number	48
Tooth tip	1.016mm
Number of turns per coil	11

Table 2.2

The stator of the machine is a big factor in machine performance. There are many parameters of the stator that must be carefully considered in order to ensure its optimum design. Following is a list of stator parameters that are considered during its design:

- Outer diameter shape
- Inner diameter/slot shape
- Winding specifications[4]

Stator winding is of high importance since incorrect configuration may lead to machine failure and improper performance, for example torque during the design process there was a mismatch in stator winding configuration which lead to the motor torque to go negative (generator action) which is the incorrect mode of operation.

2.4 Rotor design

To design the rotor of the WFSRM machine there are two types of design topologies that need to be considered. One type of rotor design topology is the salient type of rotor (figure 2.2) and the second type of design is a cylindrical type of rotor (non-salient type, figure 2.3). The salient rotor type is generally better for relatively low speeds such as in hydroelectric power generation and the cylindrical type of machine is better for relatively high speed of operation such as in steam and gas turbines. The cylindrical rotors also require low number of rotor poles in order to operate (2-4 poles). The machines with salient type of rotors require large number of poles in order to achieve the frequency of operation desired. This frequency can be theoretically calculated using the formula:

$$f = \frac{p_n N_r}{120}$$

where p_n is the number of poles, N_r is the rotor speed and f is the frequency.
The two different kinds of rotor are shown is figures 2.2 and 2.3.

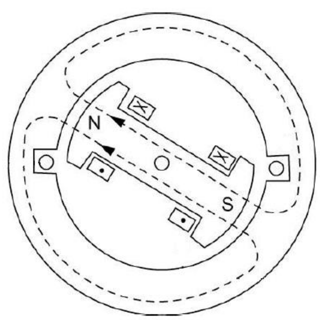

Figure 2.2

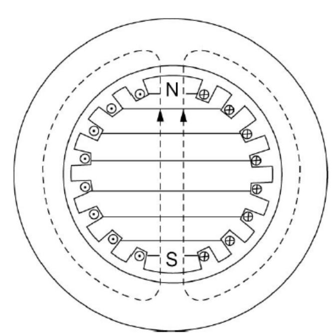

Figure 2.3

The rotor for the WFSRM was designed based on the most simple 'dumbbell' shaped rotor poles, which is of the salient type. Compared to the more sophisticated WFSRM machine rotor designs, this particular design has its advantages as it is easy to analyse, however it is much less efficient and has higher amount of power losses during operation. The rotor was design to have 8 rotor poles similar to the Prius machine.

As this rotor design is similar to the stator design since the rotor also has windings around its poles, a machine with this kind of rotor is known more generally as a wound-rotor motor. The current generated in the rotor from an external power electronic drive as shown in figure 2.4 is then passed through external resistance banks that then in effect control the overall speed of the motor by bringing it up to speed or maintaining its speed[5].

As previously discussed the flux production in the WFSRM motor will be achieved using DC excitation in the rotor using the rotor windings. A power electronic drive circuit is shown in figure 2.4 which shows the circuit layout to achieve this.

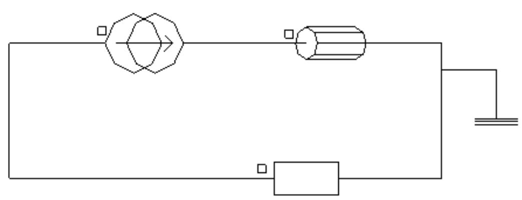

Figure 2.4

This circuit is used to produce a DC current to power the wound coils around the rotor poles. The circuit is initially powered by a 30 A current source and a large resistance and small coil conductance component is connected in series with the current source. Values of $1\times10^{9}\Omega$ was used for the resistance and 0.1 Ω. The current source value is importance as it is the biggest factor that controls the overall magnetic flux that will be produced in the machine. Another factor that influences the magnetic flux production is the number of turns of the coil winding around the rotor poles. This depends on the area that the coil windings cover and the most efficient number of turns can be calculated mathematically.

3. MOTOR PERFORMANCE CRITERIA TO BE TESTED

Several motor parameters will be tested and compared with the existing setup in the electrical vehicle in order to compare performance.

3.1 Cogging torque

The cogging torque of the motor is basically the no-current torque. It is the torque that is produced when the rotor of the machine is rotated when no load is connected to it and there is no current input. The rotation of the rotor causes friction and the movement of the rotor is not smooth. This movement is the cause of the cogging torque.

The cogging torque is sort of a general characteristic for an electromechanical energy conversion machine as a similar waveform will be obtained for both motors and generators.

The number of stator slots and rotor poles effect the cogging torque of a machine significantly. The cogging torque has no overall effect on the actual torque of the machine because at the high speeds the inertia effects cancel out any effects of the cogging torque.

Even though cogging torque is known as no current torque, the WFSRM machine design still requires some form of current excitation in the rotor for flux production (figure 2.4) without which there would be no cogging torque. However the stator windings will still have no current supplied to them [6].

3.2 Back EMF

The back EMF for the WFSRM will be tested on flux 2D. An external motor drive will be used to drive the machine. The machine will be run at 1000rpm during the simulation. The stator slots will be replaced with coil conductors. The drive circuit that will be used is shown in the figure 3.1:

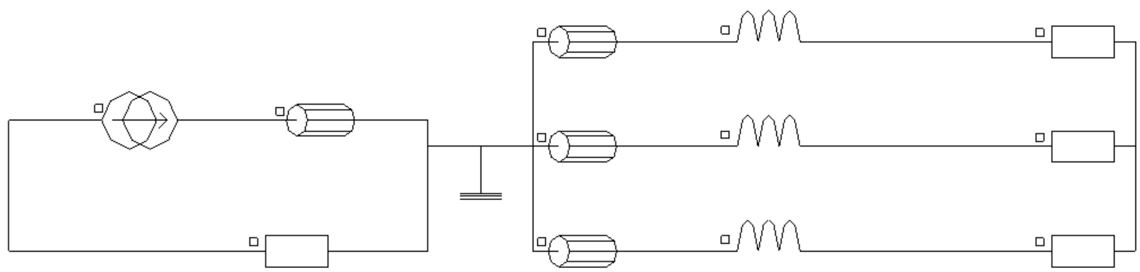

Figure 3.1

Note that the first half of the circuit is same as the one shown in figure 2.4, this circuit will supply DC current to the rotor windings. In the second half, the resistances represent the load of the generator. The inductances and coils correspond to the stator coils. High values of resistance will be used in order to calculate the back EMF for the machine.

One practical use of the back EMF is to indirectly calculate the speed of the rotor and its position. Back EMF also affects the overall efficiency of an electric motor quite considerably, because the back EMF can be thought of increasing the apparent resistance of the circuit due to the opposing voltage it is producing. One feature of an electric motor is that they consume less power when spinning compared to starting up or changing direction, in order to maximise this effect stator and motor coils use materials that have low resistivity like copper. The materials used for motor design should contain as low amount of iron in them as possible and instead contain materials with high hysteresis like steel.

3.3 Torque

The torque of an electrical motor is one of its most important characteristics. The torque of the motor is directly related with the amount of mechanical power output it would produce.

The torque of an electrical machine can be calculated using equation 3.1 shown:

$$T = \frac{\pi}{2} D^2 LBQ \qquad (3.1)$$

where T is the torque, D is the rotor diameter, I is the current, L is the rotor axial length and B is the magnetic loading.

Torque is also related directly to the mechanical power production of the machine using equation 3.2:

$$P = T\omega_r \therefore P = \frac{\pi}{2} D^2 LBQ\omega_r \qquad (3.2)$$

where ω_r is the angular speed of the rotor[7].

From this data it can be said that the higher the torque, the greater the mechanical power of the machine. Also angular speed of the rotor also affects the motor performance.

The power electronic drive shown in figure 3.1 will be modified in order to include a symmetric 3-phase sine current system which will give three sinusoidal current inputs displaced from each other by 120^o to the stator windings. The phases of these currents must correspond with the phases of the back EMF with respect to each phase. If this is not done the motor may not perform as desired and in some cases during simulations the machine performed as a generator (i.e. the torque production was negative) due to this error and hence it is very important to match the phases. Figure 3.2 shows the modified drive circuit used for the torque calculations.

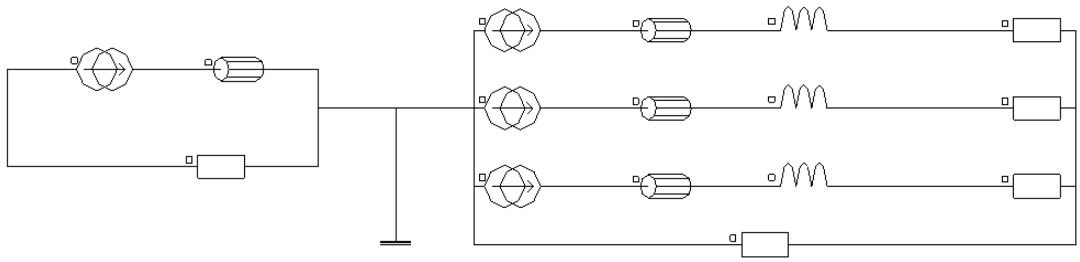

Figure 3.2

4. SIMULATION OF THE DESIGN AND RESULTS

The basic design is shown in the figure 4.1:

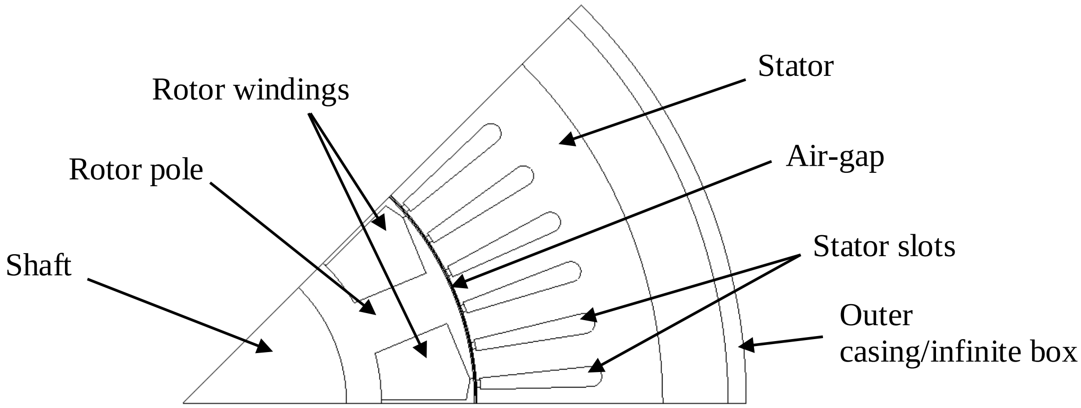

Figure 4.1

This is the geometry that is going to be simulated and tested and is the partial view of the full machine. Flux will use built-in functions to automatically produce a full circular machine during simulation. This is done to ensure accurate and fast simulations as actually designing a full machine and simulating it is a much longer process that requires a lot of computing power.

Figures 4.2 till 4.7 show various simulation results for the machine design.

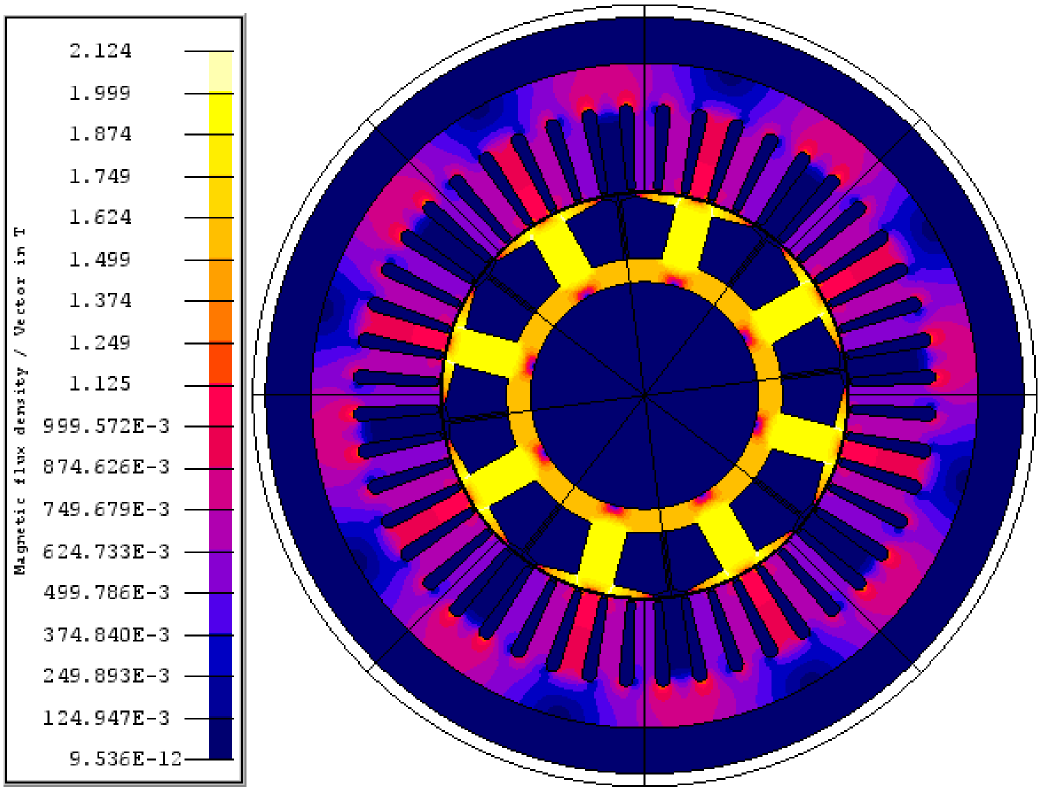
Magnetic flux density / Vector in T
2.124
1.999
1.874
1.749
1.624
1.499
1.374
1.249
1.125
999.572E-3
874.626E-3
749.679E-3
624.733E-3
499.786E-3
374.840E-3
249.893E-3
124.947E-3
9.536E-12

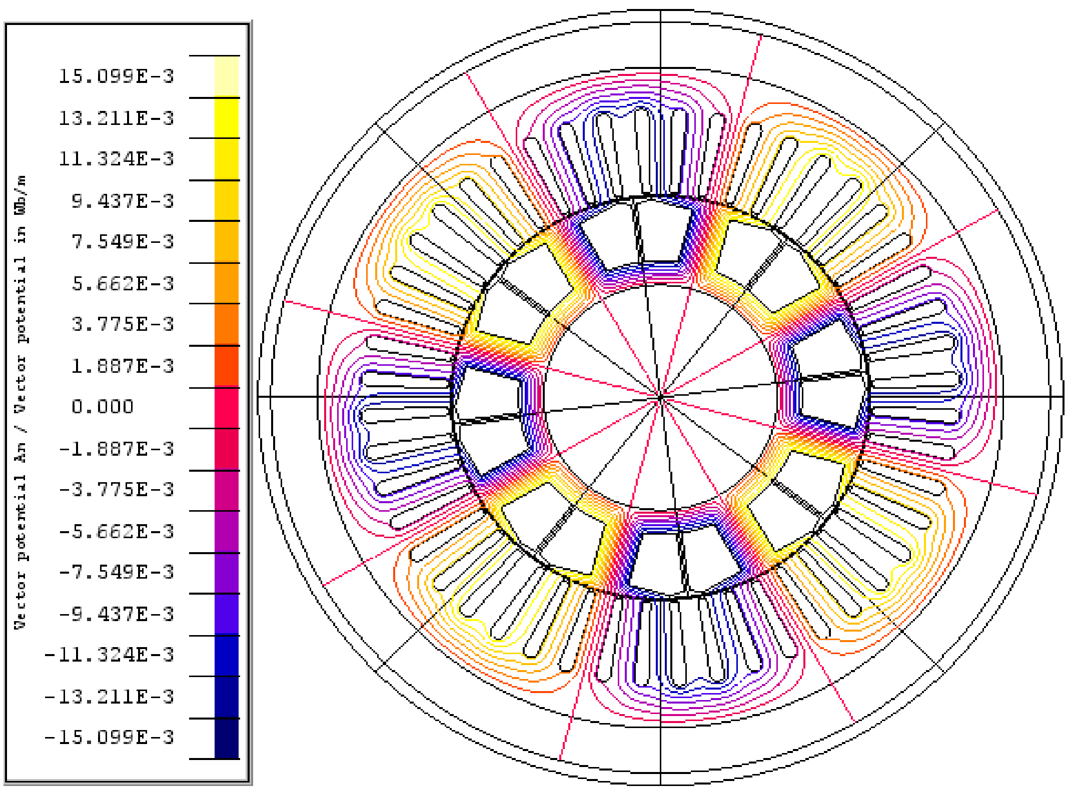
Vector potential An / Vector potential in Wb/m
15.099E-3
13.211E-3
11.324E-3
9.437E-3
7.549E-3
5.662E-3
3.775E-3
1.887E-3
0.000
-1.887E-3
-3.775E-3
-5.662E-3
-7.549E-3
-9.437E-3
-11.324E-3
-13.211E-3
-15.099E-3

Figure 4.2

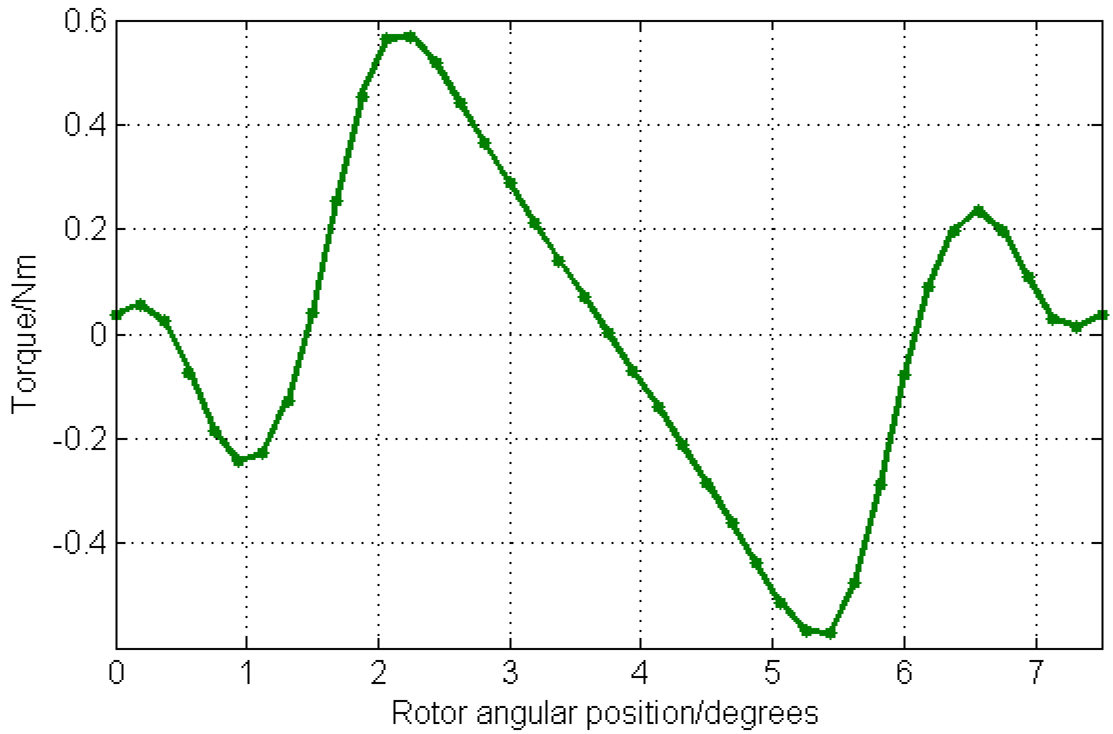

Figure 4.3

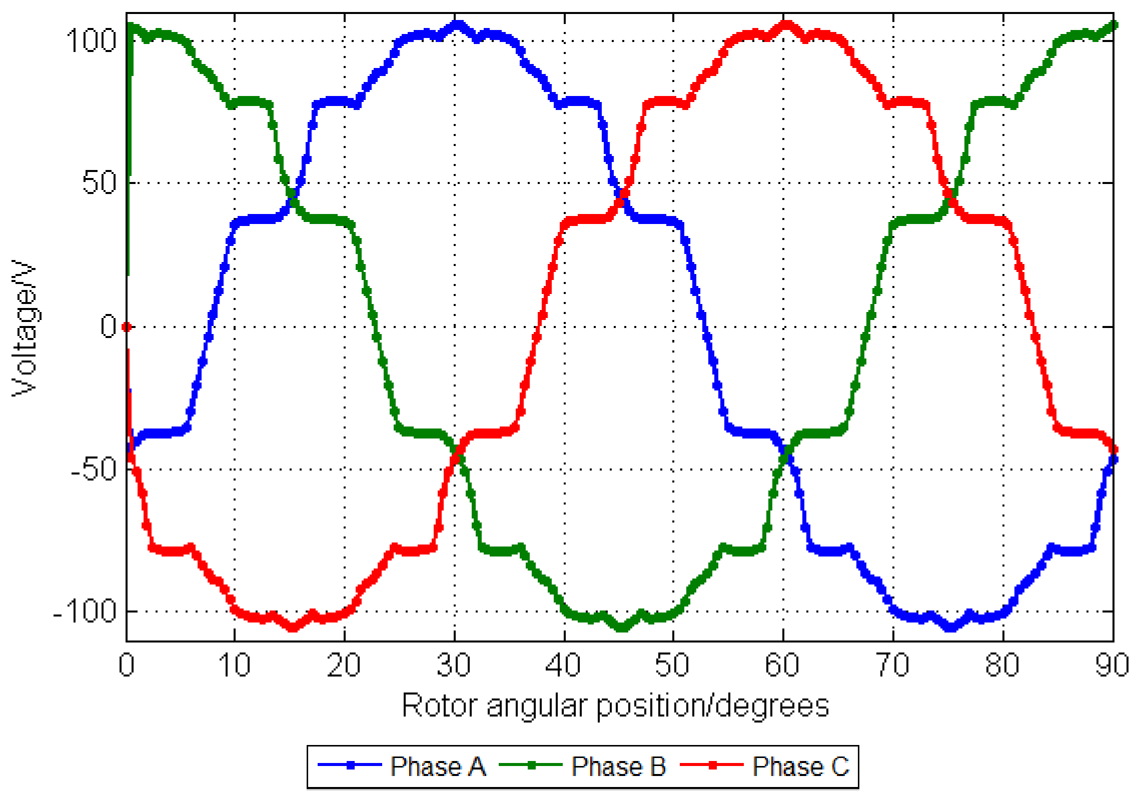

Figure 4.4

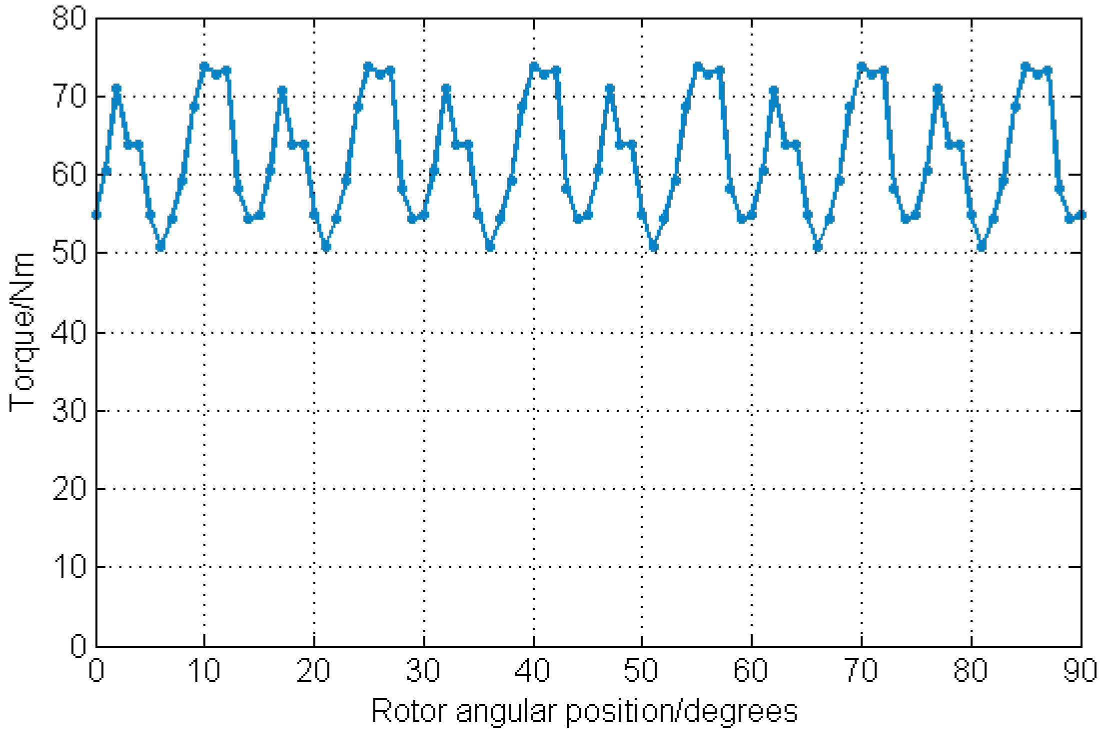

Figure 4.5

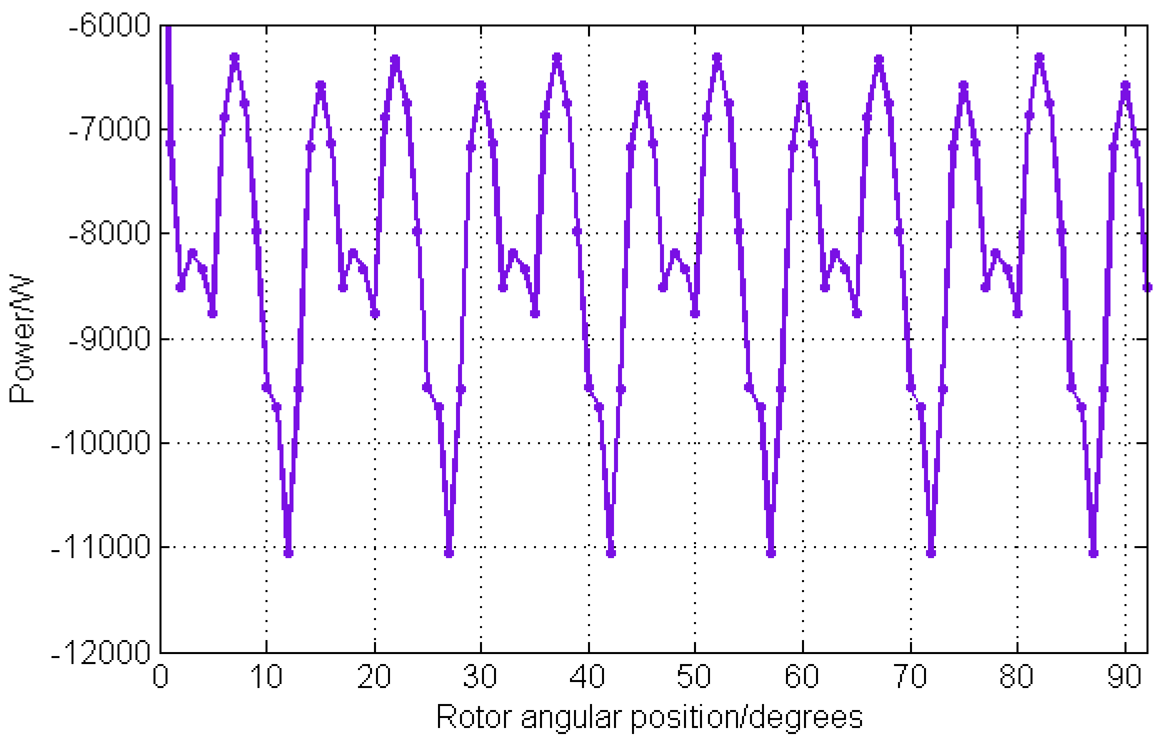

Figure 4.6

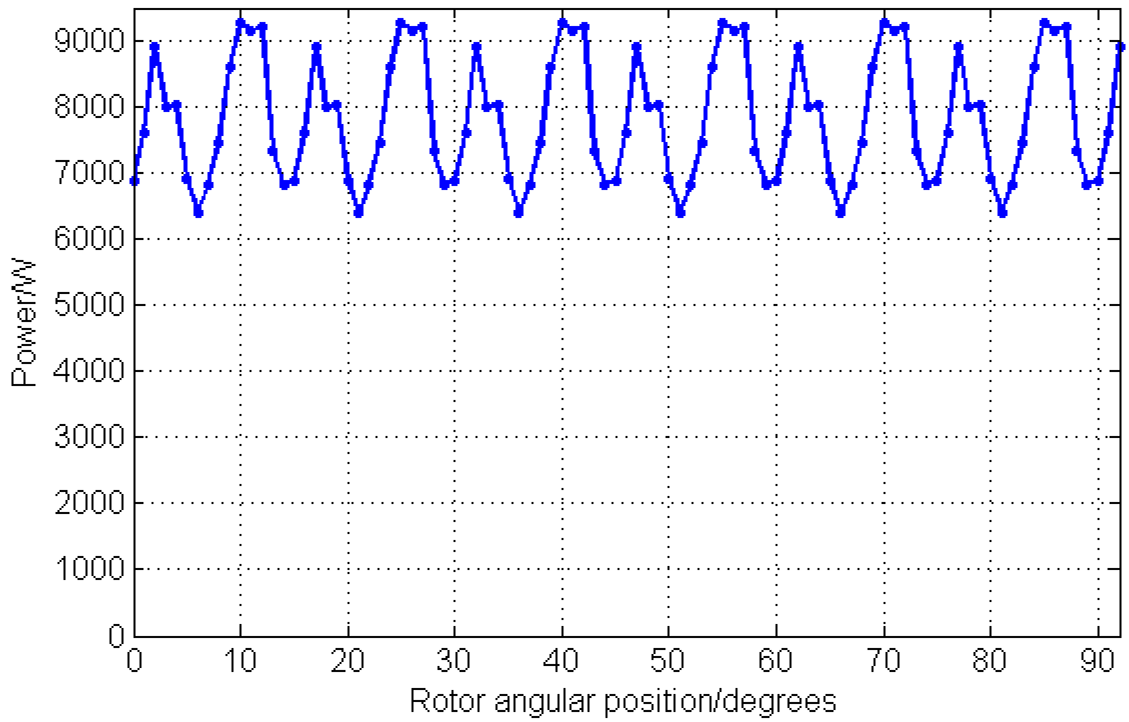

Figure 4.7

These results show the performance of the basic motor design that was employed. These results can be compared with the initial specification given for the design and that of the Prius (table 2.1). It can be seen that the rated torque of the brushless IPM motor in the Prius is rated at 207 Nm, however, the WFSRM design achieved gives an average of around 63 Nm which is about a third of the performance compared to the IPM motor in terms of torque production.

This is extremely big difference in performance. This performance drop can be explained by comparing the air-gap flux densities in both machines. For the WFSRM the air-gap flux density (B_g) is considerably less as compared to the IPM machine which is the main reason for the lower performance. This can be explained by comparing the flux densities for the two machines. The flux density distribution in the IPM motor is more uniform and dense as compared to the WFSRM flux density. This is shown in figure 4.2. From the diagram it can be seen that flux density is not distributed uniformly between the rotor and stator and in the stator it is considerably less whereas in the IPM machine it is more or less well distributed. Hence it can be concluded in order to bring the best performance of the WFSRM and hence an increase to the overall torque and mechanical power output, it is necessary to improve the flux density distribution which can be done by improving the air-gap flux density.

Motor optimization will be carried out in order to determine what changes in the initial design would bring out the best performance out of the WFSRM machine.

5. Motor Optimization

Different machine parameters will be altered and re-tested to determine the effects on the machine performance and what parameter alteration will cause a change in performance of the machine for the better or worse. Some of the factors that will be looked at are listed:

- Scaling the machine down to a smaller size
- Using a larger pole tooth width
- Removing the stator slot openings
- Reducing the pole arc width
- Reducing the air-gap length

It is important to also consider whether or not these changes are economical. The original WFSRM machine design was the best design in terms of being economical and also performance.

5.1 Machine performance when design is scaled down

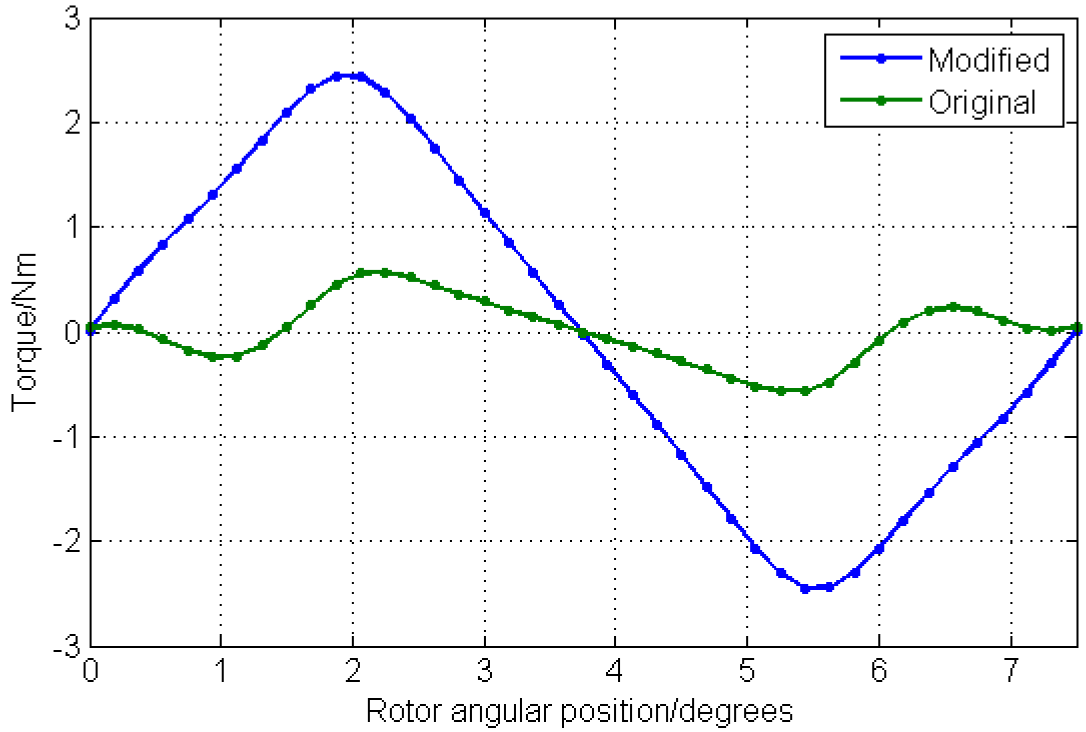

Figure 5.1

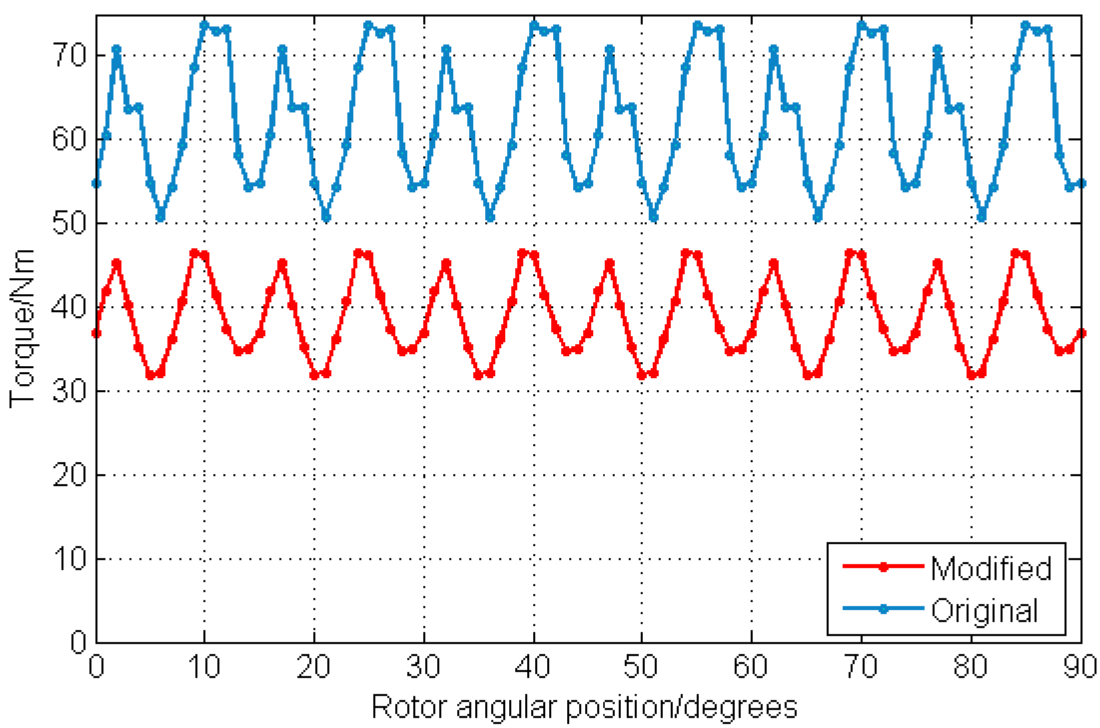

Figure 5.2

Firstly, the original rotor design will be reconfigured, more accurately, scaled to a smaller size in which the outer diameter of the rotor is changed to 120mm. The results along with the results of the original WFSRM will be compared to see how the design be optimized.

Figure 5.1 shows the cogging torque comparison between the original and the new design with the rotor inner diameter set at 120mm. From the results it can be deduced that the smaller machine has a much higher cogging torque which is more 'symmetrical' compared to that of the original WFSRM machine. This is undesirable as it has an effect on the machine performance due to friction created in the air-gap between the rotor and stator and since the overall cogging has increased considerably a smaller machine design is undesirable.

Figure 5.2 shows the comparison of torque production by both WFSRM machines. From the figure it can be deduced that the machine with a smaller size will produce a lower torque. This also confirms the theoretical deductions that state that machine volume is directly related to the torque production capability of the machine. The smaller machine however shows a smoother waveform for the torque compared to the original design. This is due to a smoother counter-EMF waveform for the smaller machine compared to the original. A smoother counter-EMF may be caused due to the more uniformly distributed magnetic flux in the smaller machine as compared to the original WFSRM, therefore in some aspects the smaller machine has its advantages. However in the long run it is better to design a slightly larger machine and check for performance increases and whether those performance increases are more beneficial as compared to the increase in cost for a larger machine.

One important improvement seen in the smaller machine was a much more uniform flux density distribution as compared to the original WFSRM. By comparing the two designs it is concluded that the flux density distribution is affected most by two factors:

1. The amount of DC current input to rotor coils
2. The size of the stator core

A smaller stator core length and a small increase in current can help improve the magnetic flux density and hence the overall machine performance. This was concluded because although the machine was scaled down, the DC current input remained unchanged at 30A in order to see what affect it has on the flux density (see Appendix 2).

5.2 Machine performance when pole tooth width increased

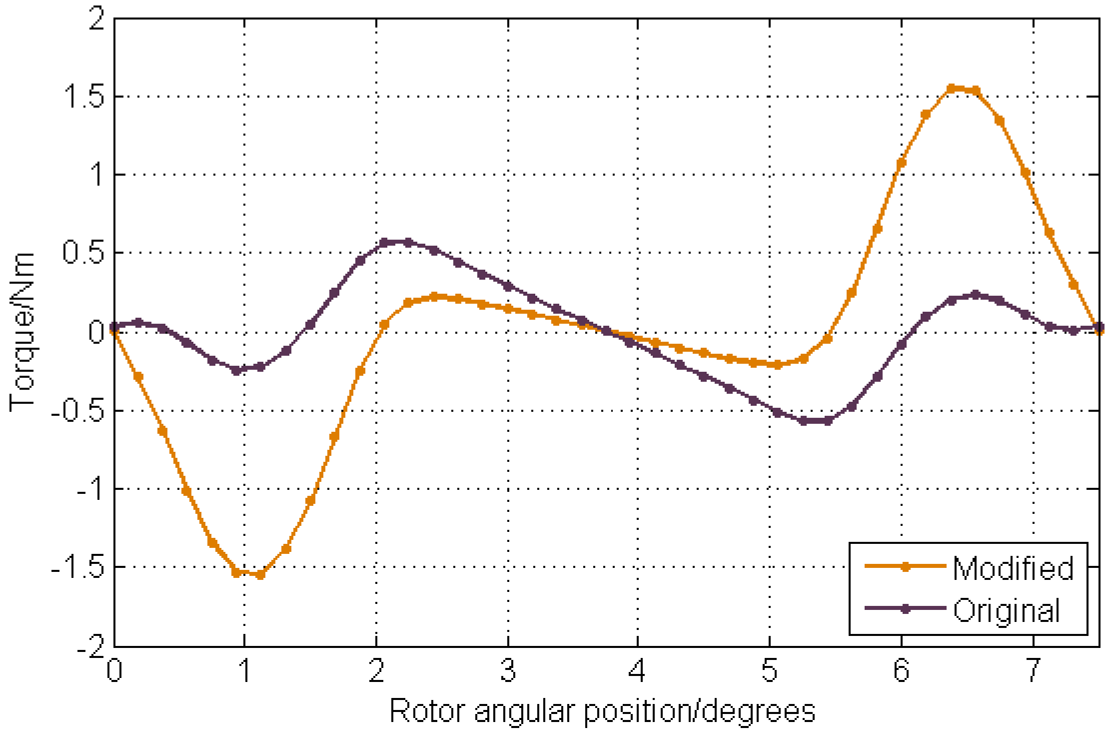

Figure 5.3

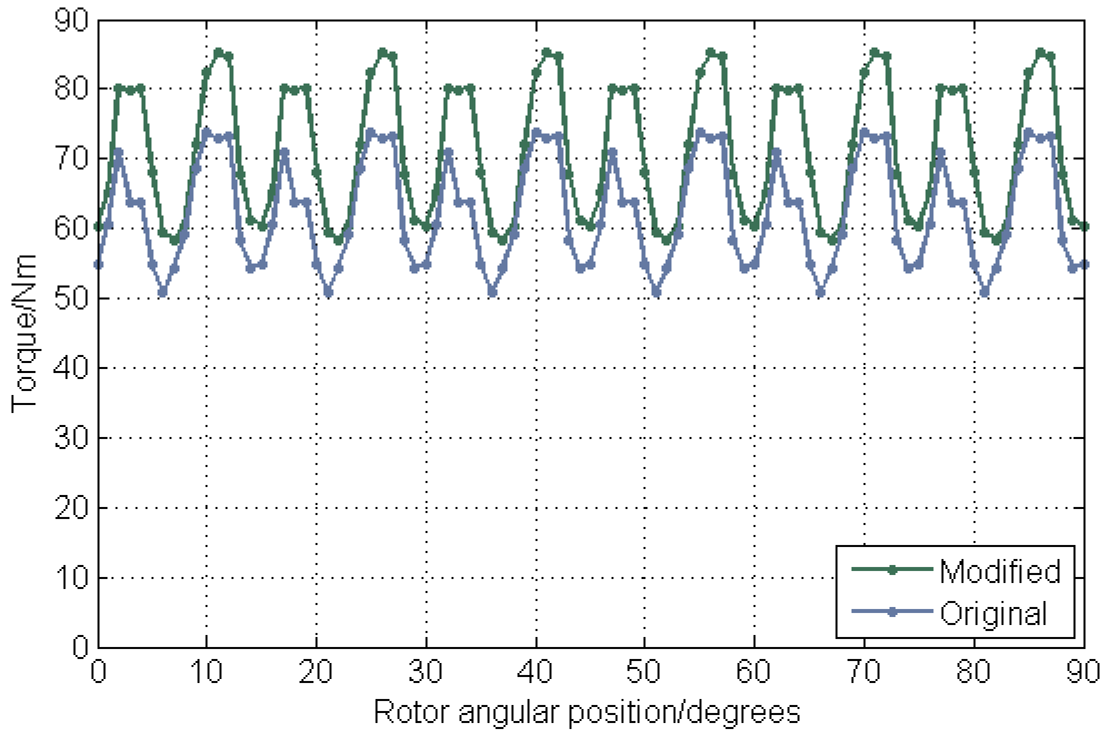

Figure 5.4

From the results in figures 5.3 and 5.4 it can said that a machine with a larger pole width would cause the cogging torque be more distorted and larger in value, however, this design also provides a larger torque output which is desirable. This means that increasing the pole tooth width is overall beneficial, however, this will make the machine more expensive overall to produce due to the higher amount of material needed to construct the machine.

Further disadvantages are the increased flux leakage in a machine with a larger pole tooth width. During optimization it necessary to consider balance between performance and cost. Overall performance has increased but so has the cost, however overall the performance increase outweighs the cost increase so increasing the pole tooth width is beneficial

However it would be better if a slightly smaller pole tooth width is used, for example 2.5mm instead of 4mm and the original 1mm design. This will result in a torque output increase with minimal increase in cost as well as result in a manageable flux leakage in the device. Overall this design has no effect on the distribution of flux density.

5.3 Machine performance in which stator slot openings are removed

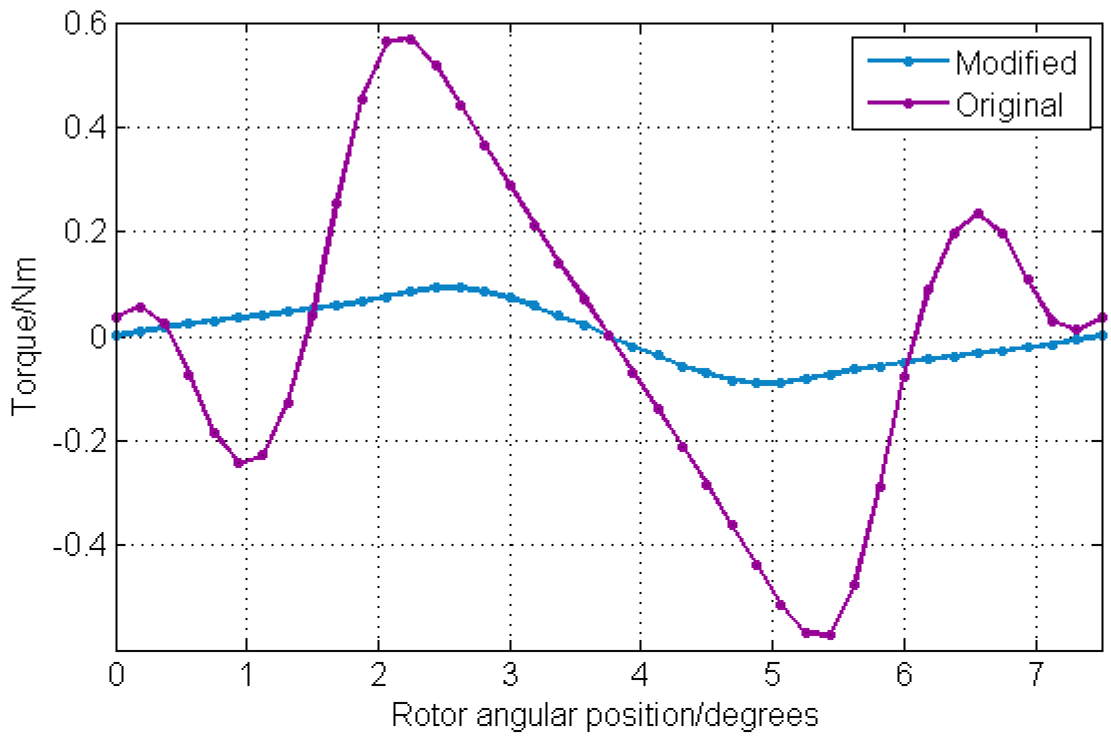

Figure 5.5

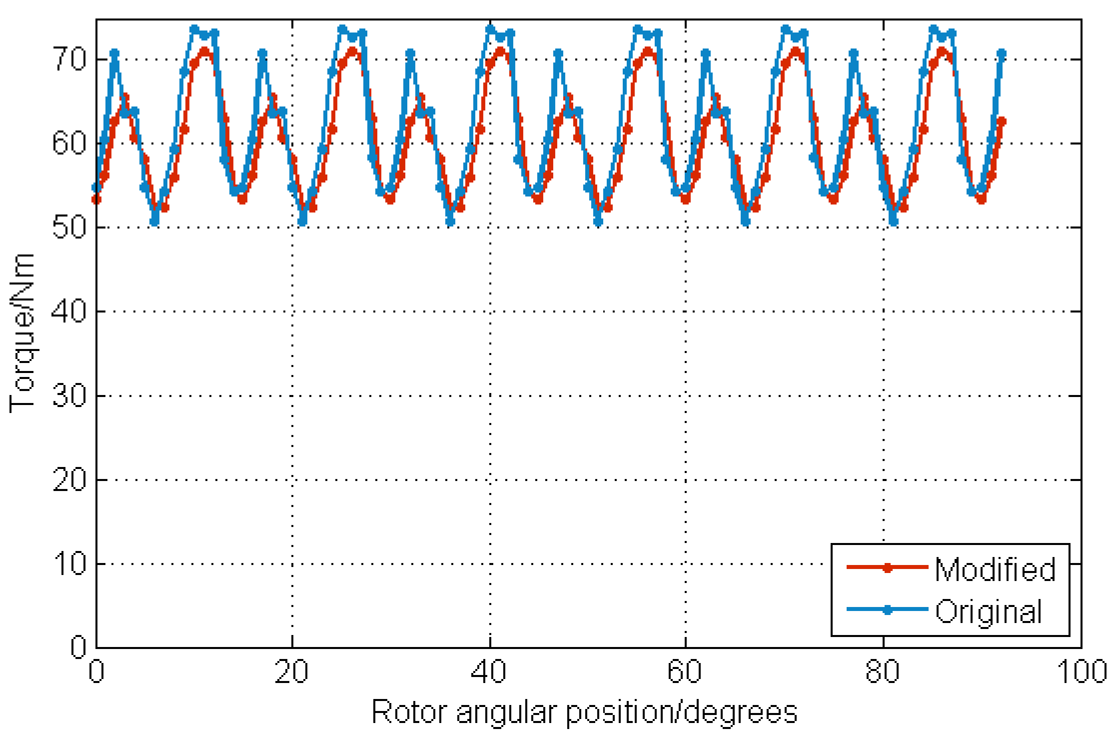

Figure 5.6

Stator lamination design without containing any slot openings is normally more beneficial to larger machine types like the wind turbine. However, it is still interesting to note the performance changes due to its removal and why this is not as beneficial to smaller machines.

From figures 5.5 and 5.6 it can be seen that for a machine design in which the wedge is removed from the stator lamination, the cogging torque becomes almost non-existent and also the average torque production in the machine is almost the same. Also the counter EMF voltages also form a smoother waveform for this modified WFSRM machine design. However the downside to this design is the increased amount of flux leakage in the device and also the increased cost of production. Therefore overall this machine design is not beneficial, however, in the case of much larger machines for example in wind turbines this could be overall more beneficial.

5.4 Machine performance with a reduced pole pitch

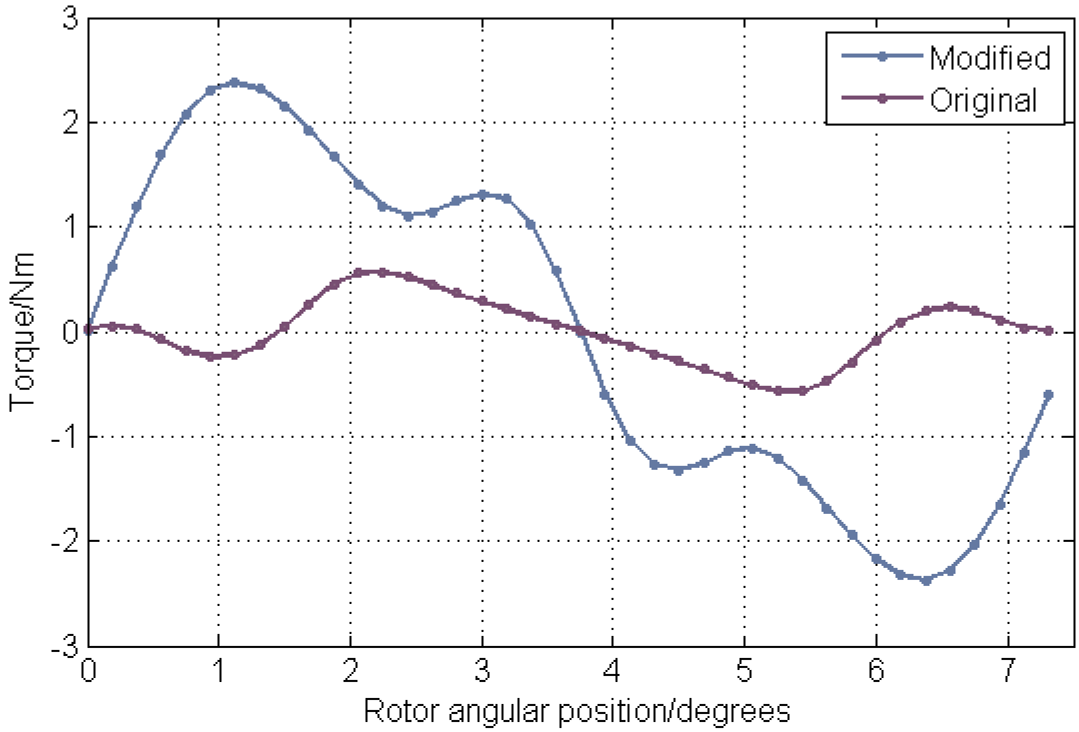

Figure 5.7

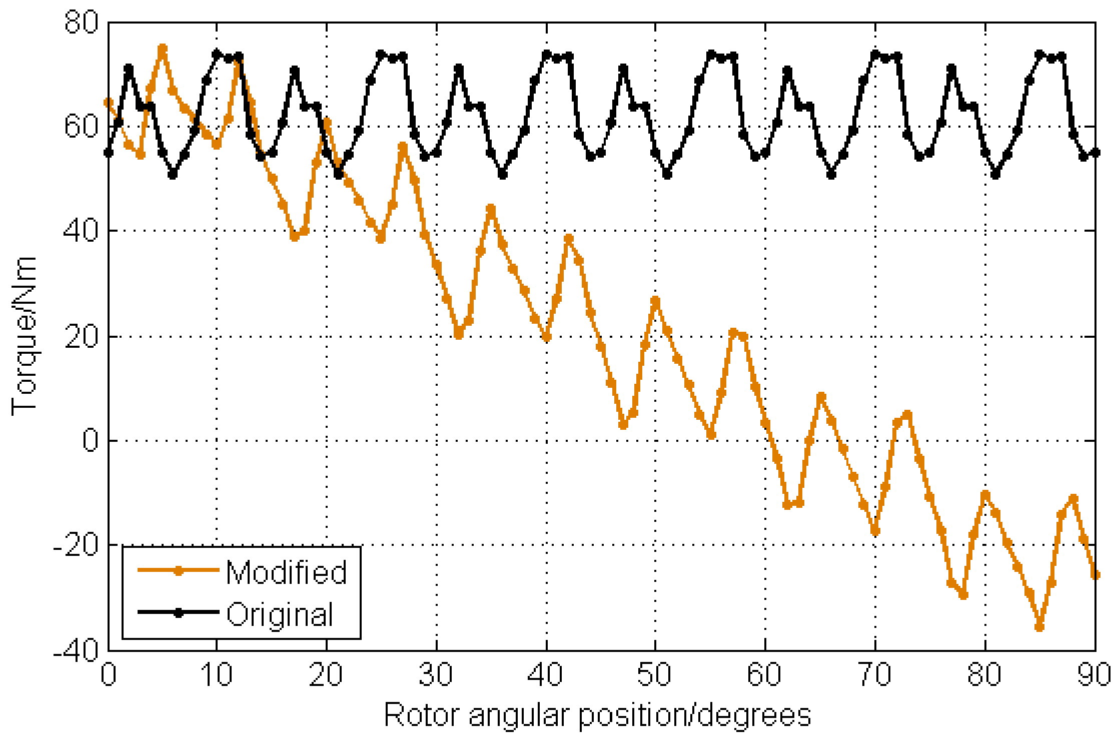

Figure 5.8

Figures 5.7 and 5.8 show the results obtained from reducing the pole pitch. The pole pitch was reduced by approximately 6^{o} and the results obtained were quite odd. The machine started correctly, however later on the machine torque drops rapidly almost as if the machine broke down or has malfunctioned using this design setup. Hence it is possible that reduction in pole pitch below an optimum value has a massive negative effect on machine performance. From these results it can be deduced that a pole pitch of a minimum 35^{o} is better and a higher pole pitch would be a better design consideration for optimization rather than a smaller pole pitch which is risky and dangerous.

5.5 Machine performance with a smaller air-gap

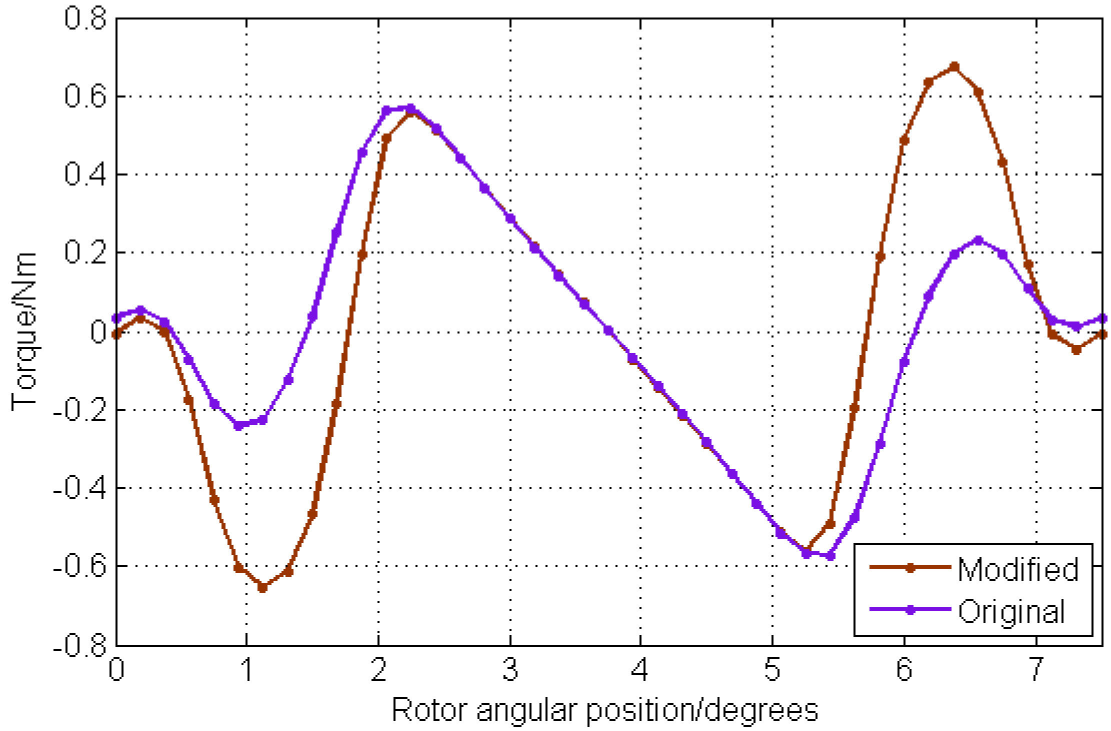

Figure 5.9

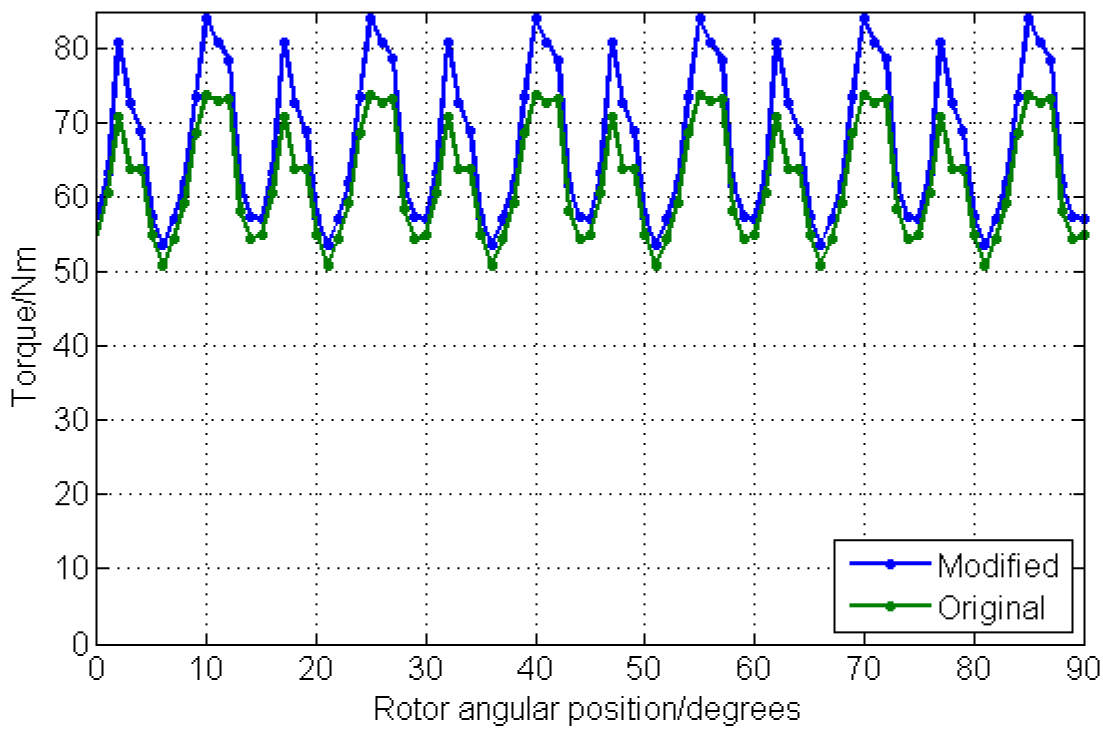

Figure 5.10

Theoretically the smaller the air-gap the higher the performance of the machine. This also increases the cost. It was investigated that how much machine performance is enhanced if the air-gap is decreased in length from 0.73mm to 0.60mm. This was done in order to conclude if the overall performance increase justifies the cost increase or not.

Figures 5.9 and 5.10 show the results obtained. From these results in can be deduced that the smaller air-gap does indeed have a significant effect on the machine performance, not only has the torque production increased but also the overall magnetic flux density distribution in machine is improved and also the overall mechanical output power. However as stated the downside is the cost increase and therefore it is necessary to determine whether this performance increase is required. If so then the air-gap must be chosen as such to put a balance between performance desired and manageable cost.

Reducing the air-gap will also improve the air-gap flux density in the machine which in turn improves the flux density distribution so a slightly smaller air-gap is a viable design optimization factor.

6. Software Issues

There were some software related issues which are mentioned in this section in order to help in the future to those working on Flux 2D. Some of them were minor errors and mostly caused due to user error, however, there was one major software error called linked mesh line error due to design periodicity. The nature of the problem and its fix is discussed in this section.

The linked mesh line error was the error that was very prominent during the course of the project and is related directly with two things; the infinite box which sets the boundary condition and the periodicity setting which sets the number of times the design is repeated, since a 45^{o} segment was used for simulations the periodicity was set to repeat the design 8 times and hence the software interpret this as a whole 360^{o} machine.

The addition of an infinite box caused problems when the periodicity was set but not when the infinite box was removed. In the same sense if the periodicity setting was removed the simulation itself ran but the results produced were incorrect. The removal of the infinite box also allowed simulation to run but also gave incorrect results. This problem was solved during the very end of the project duration and was directly related to the geometry of the design.

Figure 6.1 shows the geometry of the WFSRM machine which was produced on the sketcher in Flux 2D.

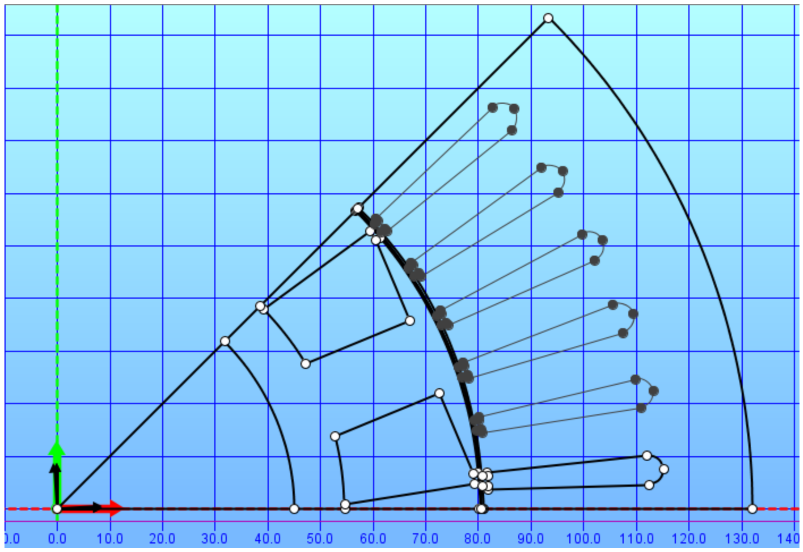

Figure 6.1

This geometry was created in two parts. One part consisted of the geometry of the stator and one part consisted of the rotor geometry. Now the problem itself lied in the construction of the geometry. Flux uses a Python script in order to translate the geometry. The script itself has an error in the way it interprets how the lines are connected to the points shown in figure 6.1. This problems are not identifiable in the sketcher. However the problems solution was found using the sketcher. If one of the lines were to be deleted in the stator, it would cause some part of the rotor to be deleted which is extremely strange since these two parts were made separately. This is shown in figure 6.2.

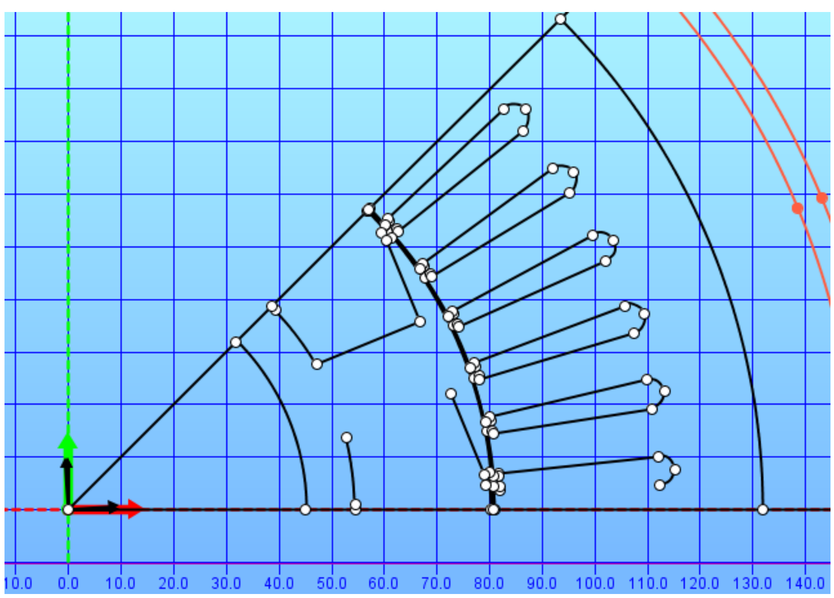

Figure 6.2

This phenomenon is the root of the problem that is then apparent by trying to define the boundary condition. The boundary condition in turn is incorrectly defined due to the apparent relationship between the rotor and stator geometries and hence the software prevents simulation of the design.

The method to fix this problem is to either check the Python script for errors in the geometry which is the hardest method and is not recommended. The easiest way is to use AutoCAD to make the design and then import it into the software. This way a very simplified version of the geometry is created and the Python script has no information stored in it that relates the points and lines of the geometry to each other. To conclude the geometry should not have its lines linked with other lines otherwise the design may not be simulated and hence the name as given by the software, *LINKED_MESHLINE ERROR*.

7. Recommendations

Further study that could have been done if time allowed was to further try to optimize the WFSRM design. Factors like the number of poles and stator slots of the machine could have been varied. Furthermore as mentioned before the machine design topology employed for this thesis was a dumbbell shaped rotor topology which is of the salient type. This is the simplest kind of design for WFSRM machines. It would be much better to have employed the more complex rotor topology shown in figure 7a as it would have had a higher efficiency and performance and this design might have been much more close to the original brushless IPM machine design that was chosen by Prius in terms of performance.

Figure 7a

Other optimization factors were also to increase the stator slot area, varying the stator wedge width and reducing the shaft diameter.

These machine optimizations were prevented mostly because of the small time frame to do the project but also the linked mesh line error mentioned previously prevented any attempt to try and carry out simulations as the new designs that were made were yielding this error.

8. Conclusions

From the various results it can be concluded that using a WFSRM for traction and automotive applications is a valid design choice. However, overall this wound-field DC excited design has an overall less performance as compared to brushless permanent magnet machines. Various optimization techniques can be modelled on the basic WFSRM design in order for it to be a better machine.

From the optimizations it can be concluded

1. A slightly smaller air-gap will make the distribution of flux much more efficient and increase machine performance considerably.
2. A larger pole tooth width would increase machine performance but there are limits on how much this can be done because this increases the flux leakages inside the device.
3. A slightly larger machine would perform better in terms of outputting a higher mechanical power at any given speed.
4. Reducing the stator core width will increase the performance of the machine theoretically according to the results obtained by enabling a much better flux density distribution.
5. An increase to the pole pitch will increase the stability of the machine while running.

By applying these modifications it is possible to create a better performing machine with reasonable increases in cost. A possible design specification is shown in Appendix 7.

9. References

[1] Professor K. Mitchell, "*EEE341 Electric Power Systems*", Synchronous machines in power systems - part 1, page 3, September 2012.

[2] Muhammad H. Rashid, *Power Electronics Handbook*, 3rd edition, pgs 984-987, 2011.

[3] Professor Z. Zhu, "*EEE305 Machine Design*", Permanent magnet machines, page 1-3 February 2013

[4] Alliance winding equipment, *Design considerations to optimize stator manufacturing* [Online], http://www.alliance-winding.com/techpapers/optprocess.pdf, pages 1-4.

[5] Dr Houssem R.H.B., 2010, Umm-Al Qura University, *Introduction to Power Engineering* [Online], Available: http://uqu.edu.sa/files2/tiny_mce/plugins/filemanager/files/4300303/IPE/t1/Intorduction%20To%20Power%20Engineering%20-%204%20Generators.pdf, pages 9-13

[6] Zhu, Z.Q., (2000, December), Influence of Design Parameters on Cogging Torque in Permanent Magnet Machines, *IEEE Transactions on Energy Conversion* [Online], 15(4), pp 407-412 Available: http://ieeexplore.ieee.org.eresources.shef.ac.uk/stamp/stamp.jsp?tp=&arnumber=900501

[7] Professor Z. Zhu, "*EEE305 Machine Design*", Relationship between dimensions and rating of machines, page 2-3 February 2013

10. Appendix

Appendix 1: Design summary sheet of the 48 slot, 8-pole motor

<table>
<tr><th colspan="4">Design summary sheet</th></tr>
<tr><td>Motor name</td><td colspan="3">48-slot, 8-pole wound-field synchronous reluctance machine</td></tr>
<tr><td colspan="2">Machine layout</td><td colspan="2">Machine topology</td></tr>
<tr><td colspan="2" rowspan="9">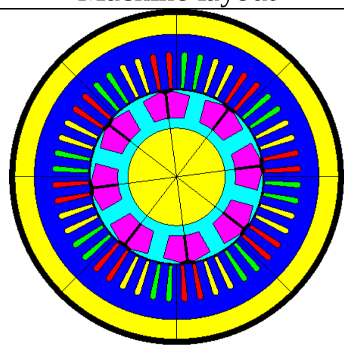</td><td>Parameter</td><td>Number</td></tr>
<tr><td>Phase number</td><td>3</td></tr>
<tr><td>Rotor poles</td><td>8</td></tr>
<tr><td>Pole pitch (mech. Deg)</td><td>35+10</td></tr>
<tr><td>Stator slot number</td><td>48</td></tr>
<tr><td>Stator coil per phase</td><td>3</td></tr>
<tr><td>Turns per coil</td><td>26</td></tr>
<tr><td>Stator slot pitch (mech. Deg)</td><td>7.5</td></tr>
<tr><td>DC current source</td><td>30 A</td></tr>
<tr><td colspan="4">Dimensions (all dimensions in mm unless otherwise stated)</td></tr>
<tr><td>Stator outer diameter</td><td>264</td><td>Air-gap length</td><td>0.73</td></tr>
<tr><td>Stator inner diameter</td><td>161.9</td><td>Mean cogging torque</td><td>1.01E-03</td></tr>
<tr><td>Rotor outer diameter</td><td>160.4</td><td>Mean torque</td><td>6.23E+01</td></tr>
<tr><td>Pole tooth width</td><td>1</td><td>Maximum Back EMF</td><td>1.06E+02</td></tr>
<tr><td>Shaft diameter</td><td>90</td><td>Minimum Back EMF</td><td>1.06E+02</td></tr>
<tr><td>Pole width</td><td>15</td><td>Outer boundary length</td><td>310</td></tr>
</table>

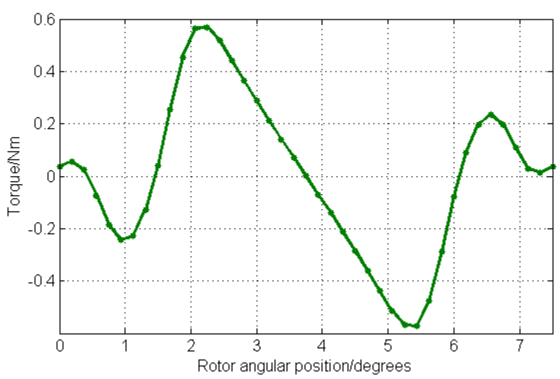

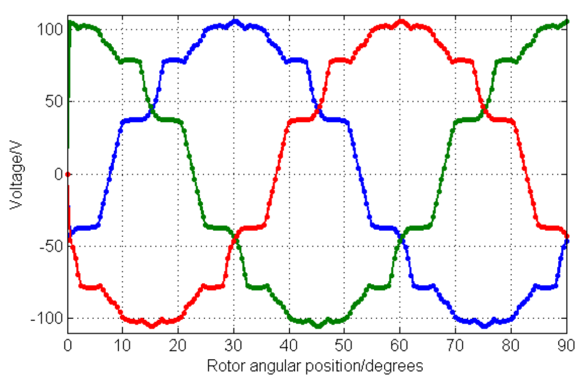

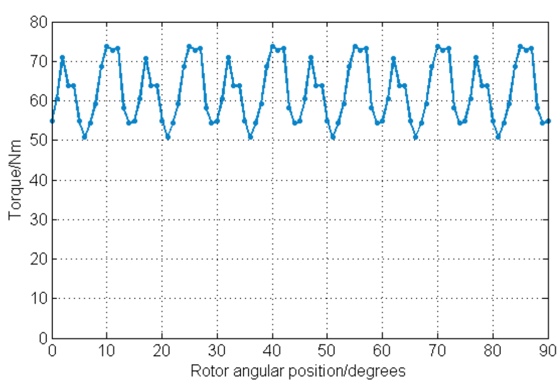

Appendix 2: Design summary sheet of the scaled down machine

Design summary sheet			
Motor name	48-slot, 8-pole wound-field synchronous reluctance machine		
Machine layout		Machine topology	
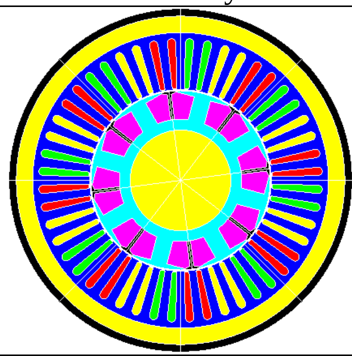		Parameter	Number
		Phase number	3
		Rotor poles	8
		Pole pitch (mech Deg)	35+10
		Stator slot number	48
		Stator coil per phase	3
		Turns per coil	26
		Stator slot pitch (mech Deg)	7.5
		DC current source	30 A
Dimensions (all dimensions in mm unless otherwise stated)			
Stator outer diameter	198	Air-gap length	0.73
Stator inner diameter	121.48	Mean cogging torque	-4.51E-03
Rotor outer diameter	120	Mean torque	3.89E+01
Pole tooth width	1	Maximum Back EMF	7.61E+01
Shaft diameter	67.5	Minimum Back EMF	-7.61E+01
Pole width	11.19	Outer boundary length	225

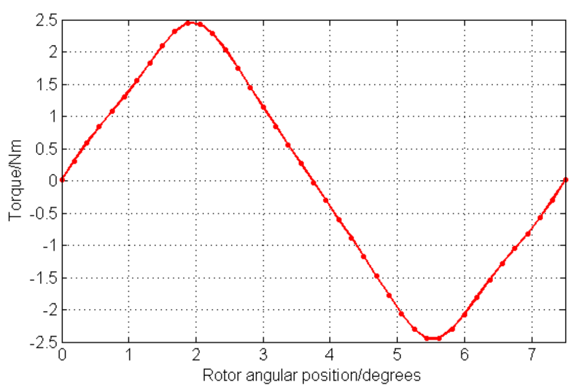

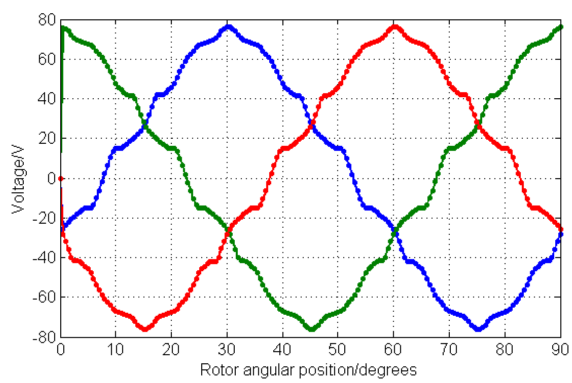

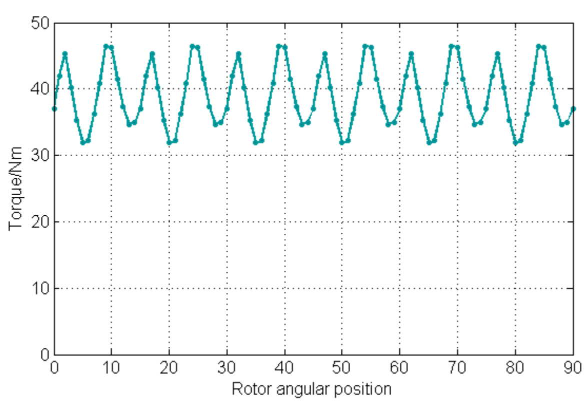

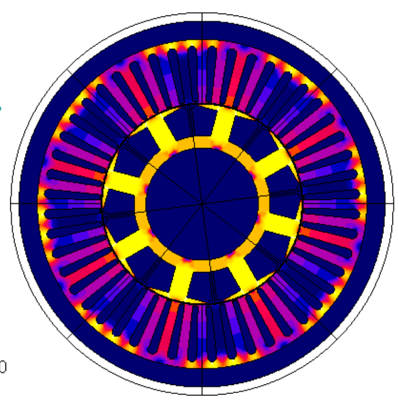

Appendix 3: Design summary sheet of tooth width modified machine

<table>
<tr><td colspan="4">Design summary sheet</td></tr>
<tr><td>Motor name</td><td colspan="3">48-slot, 8-pole wound-field synchronous reluctance machine</td></tr>
<tr><td colspan="2">Machine layout</td><td colspan="2">Machine topology</td></tr>
<tr><td colspan="2" rowspan="9">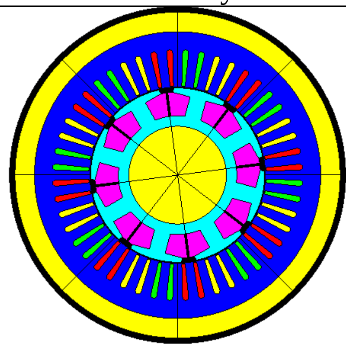</td><td>Parameter</td><td>Number</td></tr>
<tr><td>Phase number</td><td>3</td></tr>
<tr><td>Rotor poles</td><td>8</td></tr>
<tr><td>Pole pitch (mech Deg)</td><td>35+10</td></tr>
<tr><td>Stator slot number</td><td>48</td></tr>
<tr><td>Stator coil per phase</td><td>3</td></tr>
<tr><td>Turns per coil</td><td>26</td></tr>
<tr><td>Stator slot pitch (mech. Deg)</td><td>7.5</td></tr>
<tr><td>DC current source</td><td>30 A</td></tr>
<tr><td colspan="4">Dimensions (all dimensions in mm unless otherwise stated)</td></tr>
<tr><td>Stator outer diameter</td><td>264</td><td>Air-gap length</td><td>0.73</td></tr>
<tr><td>Stator inner diameter</td><td>161.9</td><td>Mean cogging torque</td><td>1.15E-03</td></tr>
<tr><td>Rotor outer diameter</td><td>160.4</td><td>Mean torque</td><td>7.09E+01</td></tr>
<tr><td>Pole tooth width</td><td>4</td><td>Maximum Back EMF</td><td>9.02E+01</td></tr>
<tr><td>Shaft diameter</td><td>90</td><td>Minimum Back EMF</td><td>-9.02E+01</td></tr>
<tr><td>Pole width</td><td>15</td><td>Outer boundary length</td><td>310</td></tr>
</table>

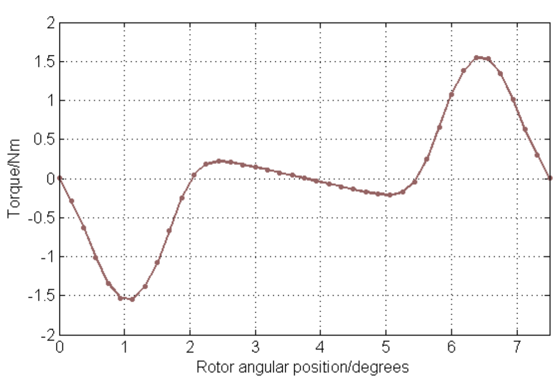

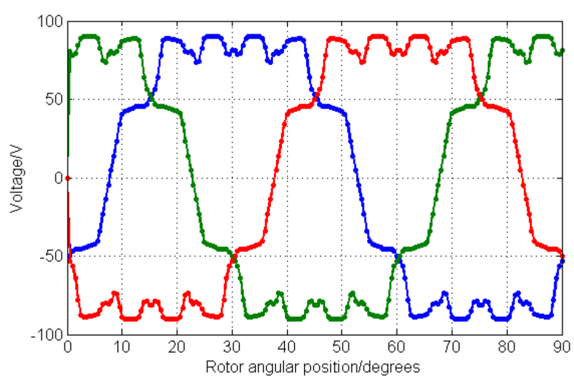

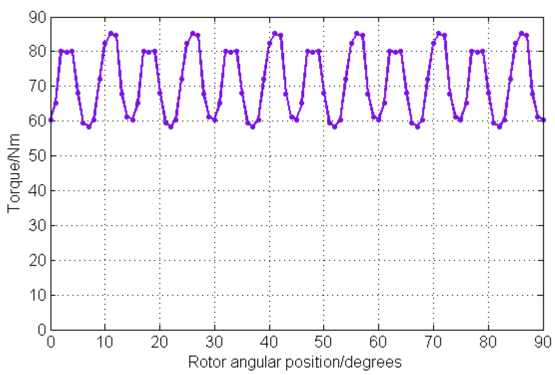

Appendix 4: Design summary sheet of machine with no slot openings

Design summary sheet			
Motor name	48-slot, 8-pole wound-field synchronous reluctance machine		
Machine layout		Machine topology	
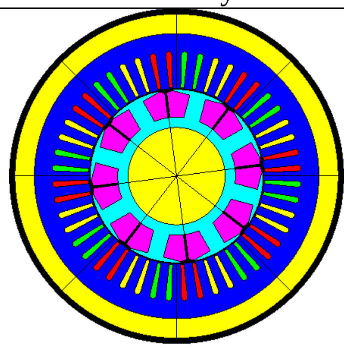		Parameter	Number
		Phase number	3
		Rotor poles	8
		Pole pitch (mech Deg)	35+10
		Stator slot number	48
		Stator coil per phase	3
		Turns per coil	26
		Slot pitch (mech Deg)	7.5
		DC current source	30 A
Dimensions (all dimensions in mm unless otherwise stated)			
Stator outer diameter	264	Air-gap length	0.73
Stator inner diameter	161.9	Mean cogging torque	8.49E-04
Rotor outer diameter	160.4	Mean torque	6.05E+01
Pole tooth width	1	Maximum Back EMF	9.28E+01
Shaft diameter	90	Minimum Back EMF	-9.28E-01
Pole width	15	Outer boundary length	310

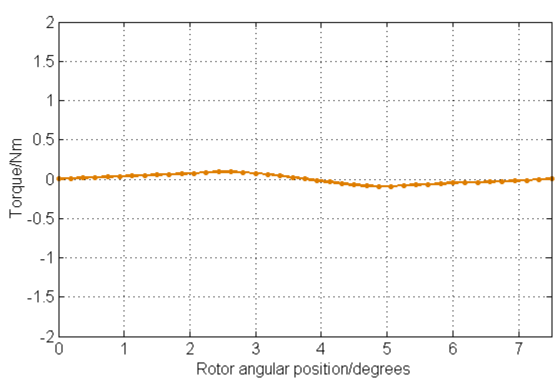

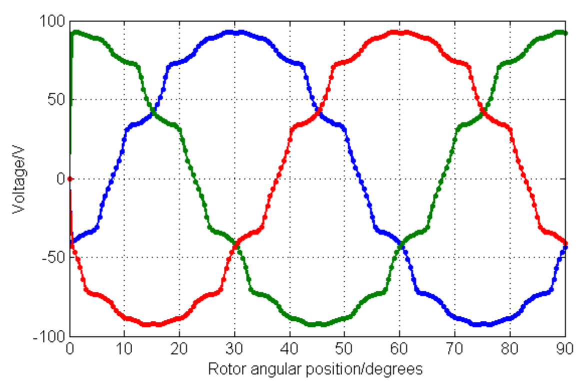

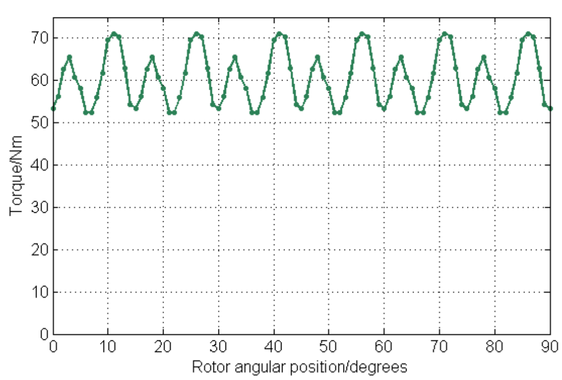

Appendix 5: Design summary sheet of machine with reduced pole pitch

<table>
<tr><td colspan="4">Design summary sheet</td></tr>
<tr><td>Motor name</td><td colspan="3">48-slot, 8-pole wound-field synchronous reluctance machine</td></tr>
<tr><td colspan="2">Machine layout</td><td colspan="2">Machine topology</td></tr>
<tr><td colspan="2" rowspan="9">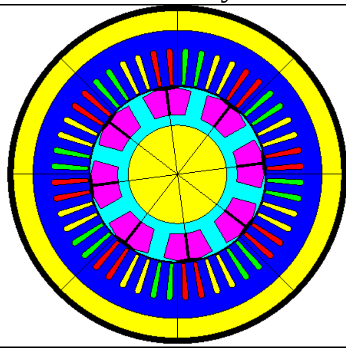</td><td>Parameter</td><td>Number</td></tr>
<tr><td>Phase number</td><td>3</td></tr>
<tr><td>Rotor poles</td><td>8</td></tr>
<tr><td>Pole pitch (mech Deg)</td><td>29+16</td></tr>
<tr><td>Stator slot number</td><td>48</td></tr>
<tr><td>Stator coil per phase</td><td>3</td></tr>
<tr><td>Turns per coil</td><td>26</td></tr>
<tr><td>Slot pitch (mech Deg)</td><td>7.5</td></tr>
<tr><td>DC current source</td><td>30 A</td></tr>
<tr><td colspan="4">Dimensions (all dimensions in mm unless otherwise stated)</td></tr>
<tr><td>Stator outer diameter</td><td>264</td><td>Air-gap length</td><td>0.73</td></tr>
<tr><td>Stator inner diameter</td><td>161.9</td><td>Mean cogging torque</td><td>1.08E-05</td></tr>
<tr><td>Rotor outer diameter</td><td>160.4</td><td>Mean torque</td><td>1.97E+01</td></tr>
<tr><td>Pole tooth width</td><td>1</td><td>Maximum Back EMF</td><td>1.36E+02</td></tr>
<tr><td>Shaft diameter</td><td>90</td><td>Minimum Back EMF</td><td>-1.36E+02</td></tr>
<tr><td>Pole width</td><td>15</td><td>Outer boundary length</td><td>310</td></tr>
</table>

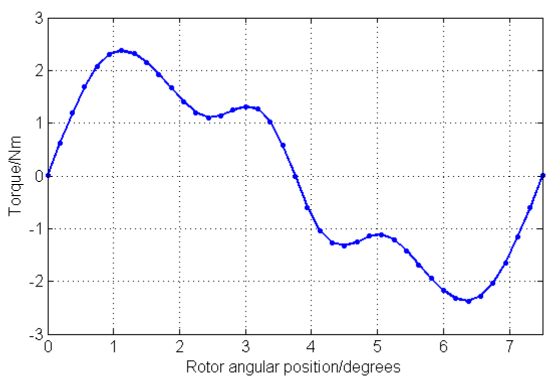

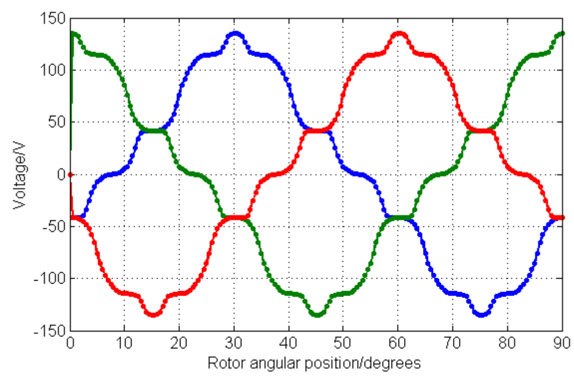

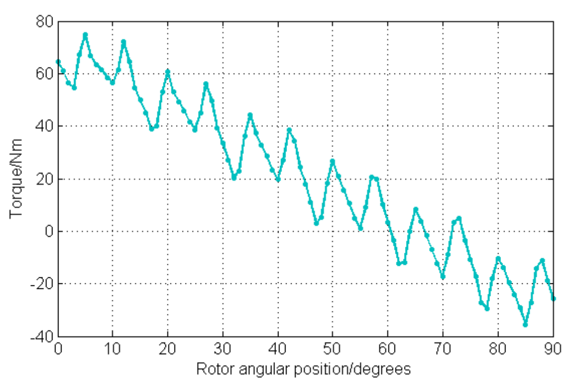

Appendix 6: Design summary sheet of machine with reduced air-gap

Design summary sheet			
Motor name	48-slot, 8-pole wound-field synchronous reluctance machine		
Machine layout		Machine topology	
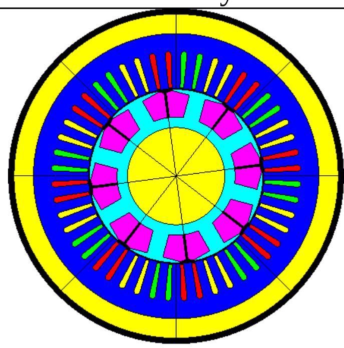		Parameter	Number
		Phase number	3
		Rotor poles	8
		Pole pitch (mech Deg)	35+10
		Stator slot number	48
		Stator coil per phase	3
		Turns per coil	26
		Slot pitch (mech Deg)	7.5
		DC current source	30 A
Dimensions (all dimensions in mm unless otherwise stated)			
Stator outer diameter	264	Air-gap length	0.60
Stator inner diameter	161.9	Mean cogging torque	9.58E-04
Rotor outer diameter	160.898	Mean torque	6.72E+01
Pole tooth width	1	Maximum Back EMF	1.05E+02
Shaft diameter	90	Minimum Back EMF	-1.05E+02
Pole width	15	Outer boundary length	310

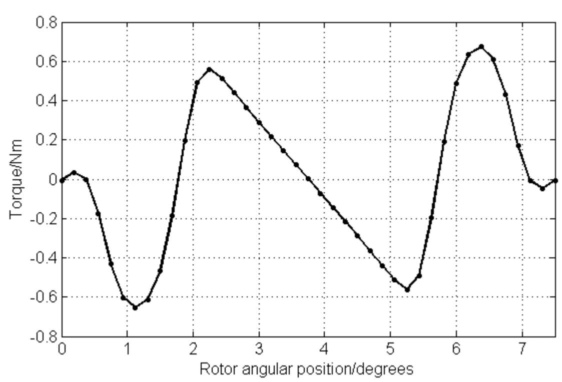

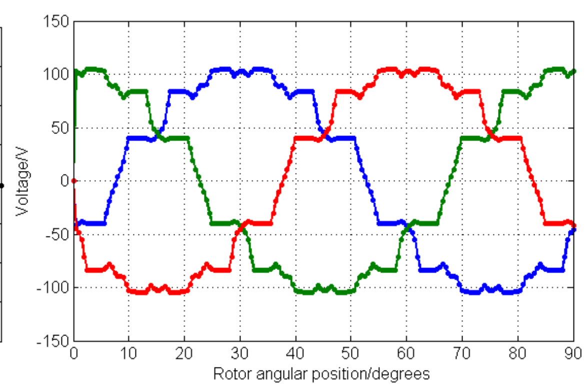

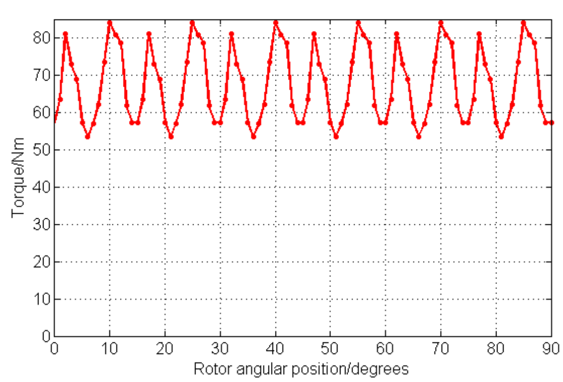

Appendix 7: Improved version of initial design specification

Parameter	***Value***
Motor diameter	290 mm
Stator outer diameter	254 mm
Stator inner diameter	161.9 mm
Number of stator slots	48
Stator construction material	Steel
Rotor outer diameter	160.92 mm
Rotor inner diameter	95 mm
Number of rotor poles	8
Rotor construction material	Steel
Shaft diameter	90 mm
Air-gap	0.63 mm
Rotor winding material	Copper
Number of turns per coil	50
DC current input to coil	30 A
Number of turns in stator winding	26
Maximum rated speed	13500 RPM
Maximum rated phase current	167 A_{RMS}
Slot fill	47%

Appendix 8: Interim Report

Design of a Wound-Field Synchronous Reluctance Motor

Abstract – In this design project it is required to design a wound-field synchronous reluctance motor (WFSRM) on Flux 2D which is a software by Cedrat®. It is required to design the motor then carry out simulations to determine various motor characteristics such as its cogging torque and back emf, in general the overall motor performance and we have to compare it with the motor performance of the Toyota Prius hybrid vehicle.

I. MOTOR DESIGN SPECIFICATION

Motor diameter	310 mm
Stator outer diameter	264 mm
Stator inner diameter	161.9 mm
Number of stator slots	48
Stator slot wedge width	1.9304 mm
Stator slot tooth width	3.1496 mm
Stator slot length	33.538 mm
Stator construction material	Steel
Rotor outer diameter	160.4 mm
Rotor inner diameter	95 mm
Number of rotor poles	8
Rotor construction material	Steel
Shaft diameter	90 mm
Airgap	0.73 mm
Rotor winding material	Copper
Number of turns per coil	50
Current input to coil	30 A

Table 1

II. GENERAL MOTOR DESIGN

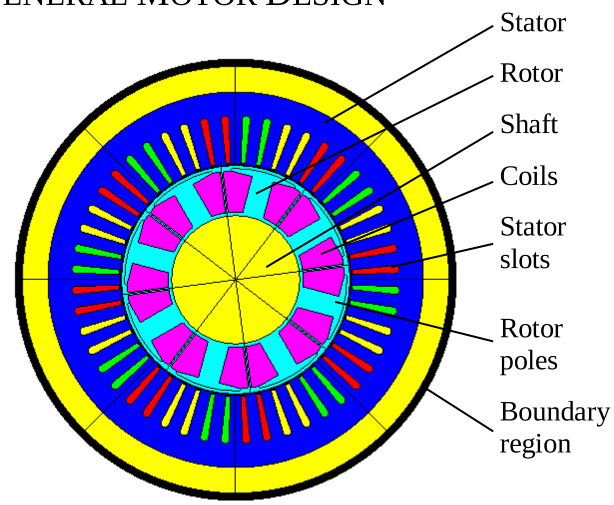

Figure 1

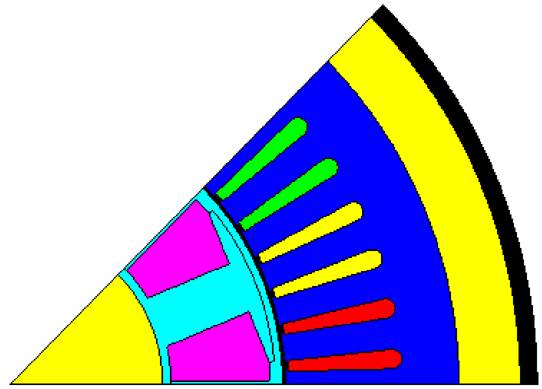

Figure 2

Figure 1 shows the design of the WFSRM and figure 2 shows part of the motor.

III MOTOR PERFORMANCE

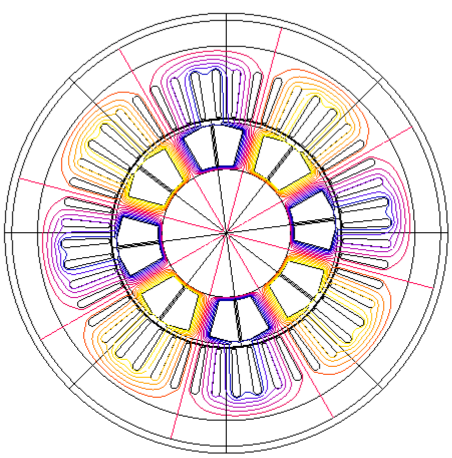

Figure 3

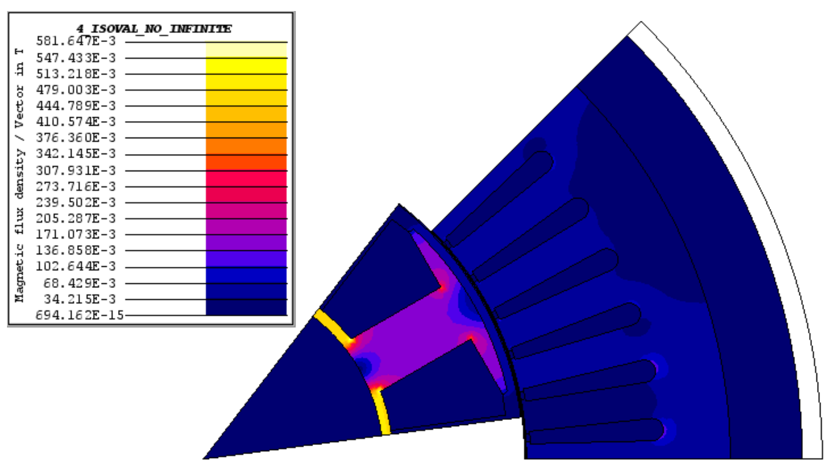

Figure 4

Figure 3 shows the simulation of flux linkage in the motor and figure 4 shows the distribution of the magnetic flux density. All these results were obtained from flux 2D using built in features of the software.

Since a WFSRM does not contain permanent magnets, an equivalent circuit is needed to power the wound field around the rotor. Figure 5 shows the circuit used.

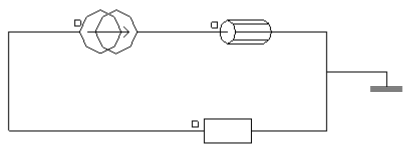

Figure 5

The accuracy of the these simulations depends on the quality of the mesh. The higher the quality of the mesh, the more accurate are the results obtained. Figure 6 shows the mesh WFSRM device. This mesh has a 99.7% number of excellent quality elements and hence a very high degree of accuracy will be obtained for our results.

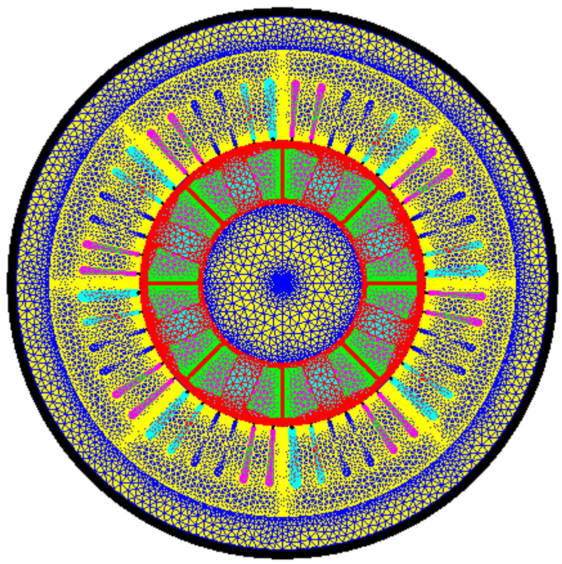

Figure 6

IV Project Starting Points

To assist us in starting the work on the design, a motor design for the Toyota Prius was given as well as tutorial sheets to help learn to use the software. The tutorial sheets helped us learn the software by making us design a induction permanent magnet motor and doing various tests such as calculating the back EMF and cogging torque on flux 2D. The motor design was used to help us understand how to design the stator and rotor, and how to assign different properties to our motor compared to the Prius machine.

V Project Progress Compared To Initial Plan

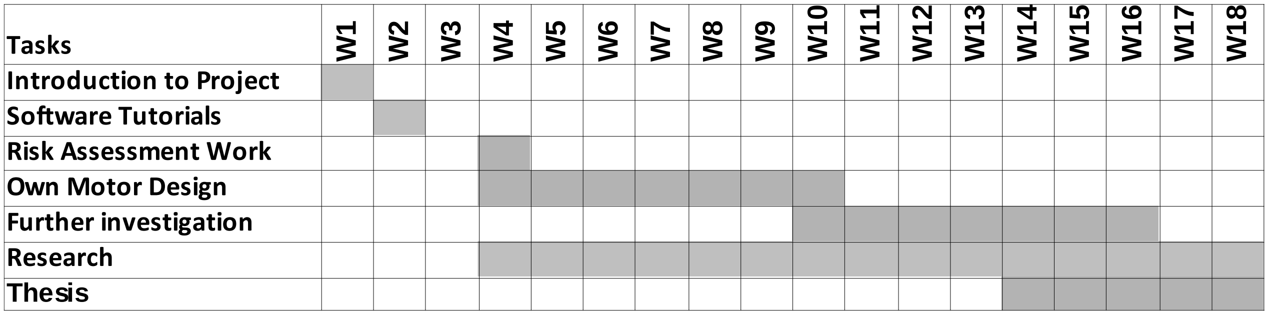

Figure 7

Figure 7 shows the initial plan for the project. So far everything that had to be done by week 12 has been done, however, there were difficulties and delays to complete the motor design, which took a week longer than expected. Hence further investigation on our motor was delayed as well, which was supposed to include tests on simulations on the motor design of various kinds such as results for different current inputs and performance difference by changing the number of rotor poles etc.